





Cite this: *J. Mater. Chem. B*, 2020, 8, 6667

## From cells-on-a-chip to organs-on-a-chip: scaffolding materials for 3D cell culture in microfluidics

John A. Terrell,  Curtis G. Jones, Giraso Keza Monia Kabandana and Chengpeng Chen \*

It is an emerging research area to integrate scaffolding materials in microfluidic devices for 3D cell culture (organs-on-a-chip). The technology of organs-on-a-chip holds the potential to obviate the gaps between pre-clinical and clinical studies. As accumulating evidence shows the importance of extracellular matrix in *in vitro* cell culture, significant efforts have been made to integrate 3D ECM/scaffolding materials in microfluidics. There are two families of materials that are commonly used for this purpose: hydrogels and electrospun fibers. In this review, we briefly discuss the properties of the materials, and focus on the various technologies to obtain the materials (e.g. extraction of collagen from animal tissues) and to include the materials in microfluidic devices. Challenges and potential solutions of the current materials and technologies were also thoroughly discussed. At the end, we provide a perspective on future efforts to make these technologies more translational to broadly benefit pharmaceutical and pathophysiological research.

Received 15th March 2020,  
Accepted 12th June 2020

DOI: 10.1039/d0tb00718h

rsc.li/materials-b

### Introduction

There are immediate needs to develop reliable tissue models for pre-clinical research. It costs \$2.5 billion and 10–15 years on average to bring a drug to market.<sup>1</sup> To decrease the cost of drug development, it is critical to improve the predictive power of

pre-clinical screenings for excluding ineffective/toxic candidates as early as possible (so called “fail early, fail cheaply”).<sup>2</sup> Currently, the typical workflow in pre-clinical tests is to screen drug candidates on statically cultured cells followed by animal (e.g. rodent) experiments. However, both models have inherent limitations. Although static cell culture experiments are simple to conduct, this method only applies a monolayer of cells in a container. For most studies this does not adequately recreate the tissue/organ-level cellular complexity and 3D microenvironments (e.g. extracellular matrix, ECM), making many

Department of Chemistry and Biochemistry, University of Maryland Baltimore County, 21250, MD, USA. E-mail: cpchen@umbc.edu; Tel: +1-410 455 3053



John A. Terrell

John completed his undergraduate studies in chemistry at Virginia Tech in Blacksburg, Virginia. After graduating, he worked at a contract research organization which provided services to a variety of industries, and with an emphasis on polymers, primarily assisted clients with submissions to the FDA for biomedical devices. John's interest lies in on-chip 3D cell culture, and coupling microfluidics with other instruments such as mass spectrometry to enable near real-time analyses in response to external stimuli.



Curtis G. Jones

Curtis is a second-year PhD student pursuing his degree in the field of analytical chemistry. He graduated from UMBC in 2016 with a BS in chemistry and has returned to UMBC for the completion of his PhD. His areas of interest include microfluidics and electrochemical sensing, with a specialty in the incorporation of these techniques into bioanalytical systems. Outside of the research laboratory, he is an avid lacrosse player, playing year-round in different men's leagues.

results fail to be extrapolated to subsequent clinical trials.<sup>3</sup> Animal models provide a platform for investigations on the organ and system levels. However, these expensive, time-consuming, and low-throughput experiments may not reflect human physiology; evidence shows that small genomic differences between species can lead to major aggregated physiological variances.<sup>4</sup> Indeed, based on these models, only 1% of the efficacy and toxicity results succeed in subsequent clinical studies.<sup>5</sup>

In the past two decades, advances in microfluidic technologies have provided a new platform for culturing cells in a more physiologically relevant manner.<sup>6</sup> Microfluidics are devices with  $\mu\text{m}$ -scale fluidic channels for controlled flow in small volumes ( $\mu\text{L}$ ).<sup>7</sup> These cell-laden microfluidic devices are often referred to as organs-on-a-chip.<sup>8</sup> This technology can overcome the limitations of both static cell cultures and animal studies:<sup>8–10</sup> (1) the inherent continuous flow in microfluidic devices enables continuous nutrient/oxygen supply and waste removal to maintain a stable growth environment for cells therein; (2) flow manipulation can apply desired gradients to the cells, which is especially useful for dosing studies; (3) the laminar flow in microfluidic channels can mimic blood physics in capillaries – shear stress can be introduced, and multiple cell types can be connected for inter-tissue modelling; (4) human cells are commonly used to obviate the inter-species discrepancy of animal models; and (5) with precise engineering, studying a single factor is more feasible with organs-on-a-chip than in animals. Due to these unique advantages, the organs-on-a-chip technology holds the promise to lessen the gap between pre-clinical and clinical studies.<sup>5</sup>

There have been fantastic reviews focusing on microfluidic designs (e.g. on-chip pumps) for organs-on-a-chip applications.<sup>9,10</sup> In this paper, we will discuss the topic from a new perspective: the ways that cells can be cultured in microfluidics; specifically, integration of scaffolding materials as ECM to support cell growth and functions. In our opinion, the first generation of “organ-on-a-chip” devices should be called “cell-on-a-chip” because cells were cultured as a monolayer on a side of a fluidic channel or on

embedded porous membranes. Except for a few cell types, such as endothelial cells, such models do not recreate the complex 3D cell–cell interactions assisted by ECMs on the organ level. Accumulating evidence has revealed the importance of ECMs for *in vitro* cell cultures<sup>11</sup> as the 3D environment is critical to maintain cell activities and functions including proliferation, migration, apoptosis, and responses to drugs, *etc.*<sup>12</sup> For instance, Chitcholtan *et al.* observed decreased proliferation of RL95-2 and KLE cells when cultured in 3D spheroids as compared to 2D monolayers when exposed to the anti-cancer drugs doxorubicin and cisplatin.<sup>13</sup> Hakkinen reported that ECM is an essential factor controlling the migration of fibroblasts. By comparing the migration rates of fibroblasts cultured in 3D and 2D environments, fibroblasts had significantly higher migration rates in 3D matrices comprised of collagen or cell-derived matrices.<sup>14</sup> Kloss *et al.* demonstrated that apoptosis was affected by ECM dimensionality, particularly in drug-response studies, as 3D cell cultures differ in surface area to volume ratio as compared to monolayers.<sup>15</sup> Further mechanism studies revealed that integrins and cadherins on the cell membrane can sense the ECM conditions (chemical composition and physical properties such as stiffness), and transduce the information intracellularly.<sup>16</sup> Pampaloni *et al.* and Jensen *et al.* recently provided thorough reviews on the significance of ECMs for cell cultures.<sup>17,18</sup> Therefore, continuous efforts have recently been made to include ECM materials for 3D cell cultures or even co-cultures in microfluidic device. There are two main families of scaffolding materials for organs-on-a-chip: hydrogels and electrospun fibers. These will be thoroughly reviewed in the following subsections.

## Hydrogels as scaffolding materials for organs-on-a-chip

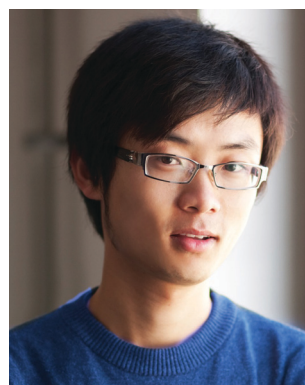
### A brief overview of hydrogels

Hydrogels are cross-linked 3D polymer networks containing large amounts of water up to 99% by weight.<sup>19</sup> Hydrogels are



**Giraso Keza Monia  
Kabandana**

*Giraso Kabandana obtained her BS from the University of Maryland, Baltimore County in spring 2018. In Fall 2018, she joined the PhD program at the same university, where she is currently working under the mentorship of Dr Chengpeng Chen with a focus on building analytical tools for biofilm culture and analysis.*



**Chengpeng Chen**

*After Dr Chengpeng Chen received a BS degree in chemistry from the Ocean University of China in 2011, he joined Dr Dana M. Spence's lab at Michigan State University as a graduate student in analytical chemistry and obtained his PhD degree in 2015. After a 3 year postdoc training with Dr R. Scott Martin at Saint Louis University (MO, USA), he became an assistant professor in the Department of Chemistry and Biochemistry at the University of Maryland Baltimore County in 2018. His research lab is interested in integrating scaffolding materials in microfluidic devices for 3D cell culture for quantitative pathophysiological studies.*

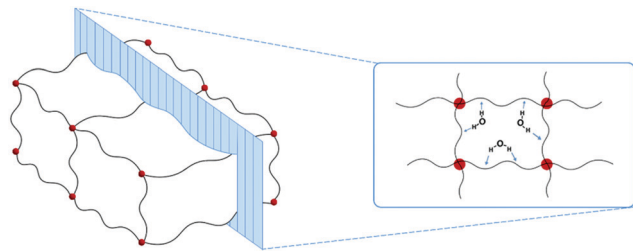


Fig. 1 Depiction of a crosslinked hydrogel and penetration of water molecules. Hydrogen bonds between the polymer backbones and water molecules make the gel porous and permeable.

permeable because of their expanded microstructure that occurs due to the affinity of the polymer backbone to the solvent (water) molecules. As shown in Fig. 1, when water penetrates the cross-linked network, the backbones are “pushed” outward to maximum due to the formation of hydrogen bonds.<sup>20</sup> The pore size of the hydrogel can be varied by altering the hydrogel chemistry and the degree of crosslinking.<sup>21</sup>

Hydrogels can be sorted into three main categories: natural, synthetic, and hybrid materials. Natural hydrogel materials directly originate from animals or plants. Animal-sourced hydrogels such as collagen are cytocompatible, present native cell-binding ligands, and exhibit chemical properties reminiscent of native tissues.<sup>22,23</sup> However, these gels usually have limited mechanical strengths, long-term stability, and batch-to-batch reproducibility.<sup>24</sup> Synthetic hydrogels, which are chemically synthesized from precursor molecules, can be more reproducibly customized to desired mechanical properties but may require additional chemical modifications for cell adherence.<sup>25,26</sup> Hybrid hydrogels are

synthesized from bio-sourced small molecules such as hyaluronic acid and amino acids. Mixtures of different types of hydrogels (copolymers) have also been utilized to complement each other's shortcomings.<sup>27</sup> Many factors should be considered when selecting a hydrogel for 3D cell culturing; the most important ones are cell compatibility, molecular diffusion rates, and mechanical properties.<sup>28</sup> There have been insightful reviews regarding hydrogel properties for cell cultures<sup>28,29</sup> and thus we will not discuss it further.

### Extraction of natural hydrogel materials from animal tissues

Native ECM molecules directly derived from animal tissue have garnered interest for 3D cell cultures.<sup>30</sup> For example, Matrigel, a hydrogel material extracted from decellularized murine tumors, has shown great success in tumor-modelling research because of the recapitulation of cancer cell microenvironments.<sup>31</sup> These molecules can be chemically functionalized and/or physically mixed with other polymers for optimal performance. Due to the high cost of such products from vendors, efforts have been made to develop protocols to extract ECM molecules, mainly collagen, from animal tissues.<sup>32,33</sup>

Collagen is the primary component of ECM in animals with two main broad types: fibrillar and non-fibrillar.<sup>34</sup> About 90% of collagen in human beings is fibrillar, the molecules of which form a triple helix fibrillar structure *via* hydrogen bonds induced by the abundant proline and hydroxyproline residues.<sup>34,35</sup> Telopeptides at both ends of a single fibrillar molecule contain a high level of lysine and hydroxylysine, which can intermolecularly form aldol crosslinks *via* the enzyme lysyl oxidase.<sup>36</sup> A schematic representation for the formation of collagen<sup>37</sup> can be seen in Fig. 2.

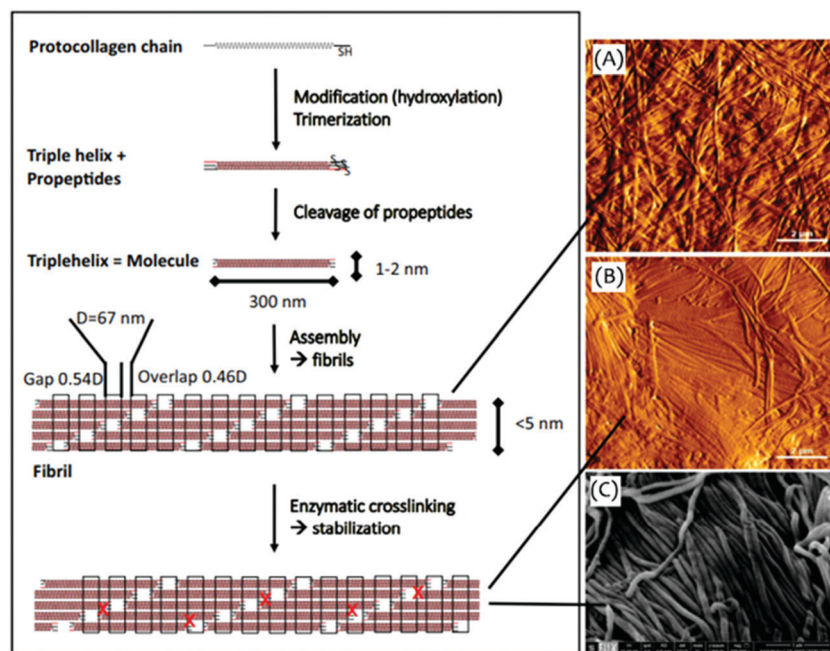


Fig. 2 Depiction of collagen formation and assembly. Atomic force microscopy images of (A) dried reassembled collagen and (B) dried porcine skin splits. (C) Scanning electron microscopy image of dried porcine skin split. Reprinted from Meyer *et al.* (2019) with permission.

Table 1 Common protocols to extract collagen from animal tissues

| Material               | Pre-treatment conditions                                                                                                                                                                                                                                     | Extraction conditions                                                                                                                                                                                                                                                                                               |
|------------------------|--------------------------------------------------------------------------------------------------------------------------------------------------------------------------------------------------------------------------------------------------------------|---------------------------------------------------------------------------------------------------------------------------------------------------------------------------------------------------------------------------------------------------------------------------------------------------------------------|
| Porcine skin           | Washed with water, cut into small pieces, and treated with 0.1 M NaOH <sup>44</sup>                                                                                                                                                                          | Immersed in 0.5 M acetic acid for 72 hours then precipitated collagen from the supernatant with 0.9 M NaCl. <sup>44</sup>                                                                                                                                                                                           |
| Silver-line grunt skin | Homogenized in 0.5 M acetic acid for 3 minutes using a Kinematica Polytron (immersion disperser) <sup>45</sup>                                                                                                                                               | Extracted and agitated in 0.5 M acetic acid for 24 hours and then centrifuged. Remaining residue was reextracted using the same procedure then treated with 0.1% pepsin <sup>45</sup>                                                                                                                               |
| Bovine bone            | Pulverized and immersed in 0.1 M NaOH for 48 hours. Rinsed with water, then a Na-EDTA solution, followed by a 10% butanol solution. <sup>46</sup>                                                                                                            | Extracted in 0.5 M acetic acid for 72 hours, centrifuged, followed by the addition of 0.05 M Tris. Precipitated in 2.6 M NaCl. <sup>46</sup>                                                                                                                                                                        |
| Emu skin               | Cut into small pieces and homogenized in 10% EtOH for 96 hours followed by lyophilization. <sup>47</sup>                                                                                                                                                     | Treated in 0.5 M acetic acid for 48 hours followed by centrifugation and precipitation of the supernatant in NaCl. <sup>47</sup>                                                                                                                                                                                    |
| Snakehead skin         | Soaked in 0.1 M NaOH containing 0.5% (v/v) non-ionic detergent (Tween 80) for 24 hours. Samples then washed with cold distilled water until a neutral or slightly basic pH was reached. Residual fat was removed by 15% butanol over 24 hours. <sup>48</sup> | Suspended in 0.5 M acetic acid with 0.02% (w/v) pepsin (250 U mg <sup>-1</sup> ) with a sample/solution ratio of 1/60 (w/v) and gentle rotation <i>via</i> orbital shaker for 36 hours. Centrifugation was then performed and collagen precipitated from the supernatant <i>via</i> addition of NaCl. <sup>48</sup> |

The intermolecular crosslinks must be broken in order to extract collagen from solid animal tissue. The most commonly used techniques for this purpose are acid/base treatment and enzymatic digestion.<sup>38,39</sup> Acids/bases are used for hydrolysis of native collagen and result in partially hydrolysed structures (gelatin).<sup>38</sup> Mineral acids, specifically acetic acid, are most often used for hydrolysis of collagen.<sup>38,40</sup> The enzyme pepsin can be applied to increase the solubility of collagen due to its ability to cleave the intermolecular aldol crosslinks of the telopeptides.<sup>38,41,42</sup> Following pre-treatment to remove cells and soluble proteins, additional steps may be performed to remove other components such as the removal of excess fats *via* butanol.<sup>43</sup> Examples of these steps are shown in Table 1.<sup>44–48</sup> The extraction conditions listed do not outline additional purification steps which may be needed (*e.g.* using dialysis to remove pepsin (35 kDa)). It is common for steps to be performed at 4 °C to prevent thermal degradation of the material.

### Integration of hydrogels in microfluidics for organs-on-a-chip

After considering the type of hydrogel to be used, the next step is to determine how to apply it. On the macro scale it is a matter of dispersing the uncured hydrogel material and then cross-linking it. However, this methodology is not suitable when micron resolution is required for biomimetic devices. Ultimately, strategies for incorporating hydrogels in microfluidic devices will be based on either fabricating a device with hollow channels and filling them with a curable hydrogel, or excising channels from a hydrogel bulk material. The technique used is dictated by the resolution and complexity of the part of interest.<sup>49,50</sup>

**Filling hydrogels in pre-made microfluidic devices.** Hydrogels can be filled in premade microfluidic devices as ECMs for 3D cell culture. For example, Virumbrales-Muñoz *et al.* investigated the ability of TNF-related apoptosis inducing ligand (TRAIL) to penetrate endothelium and kill tumor cells in a 3D collagen matrix. The microfluidic device was fabricated from polydimethylsiloxane (PDMS) *via* soft lithography. The central channel was oxygen plasma treated to promote capillary actions for spontaneous filling. Droplets of collagen (1.2 mg mL<sup>-1</sup>, see ref. 51 for details), which were previously mixed 1:1 (v/v) with the cancer cell suspension, were placed on top of the device inlet

for filling. The collagen was then polymerized for 12 minutes at 37 °C. Endothelial cells were cultured in the flow path on top of the collagen containing the cancer cells (Fig. 3A). TRAIL was introduced both in its soluble form and bound to a large unilamellar vesicle.<sup>51</sup> A similar device but with two unique hydrogel constructs was prepared by Adriani *et al.* to model the blood brain barrier and how drugs can potentially affect neurocytes and astrocytes<sup>52</sup> (Fig. 3B). Here collagen solutions with suspended astrocytes (0.6 × 10<sup>6</sup> cells per mL) and neurons (5 × 10<sup>6</sup> cells per mL) were injected directly into the device and then polymerized for 30 minutes at 37 °C. Pavese *et al.* utilized a microfluidic device with a collagen barrier separating two microfluidic channels. Similarly, cells were suspended in the hydrogel solution (5 × 10<sup>6</sup> cells per mL), injected directly into the region of interest, and allowed to polymerize for 40 minutes at 37 °C. The microfluidic channels would flow tumor-specific T-cell receptor T (TCR-T) cells parallel to the hydrogel which contained human hepatocytes. The efficacy of the TCR-T cells were then observed under different oxygen conditions and in the presence of inflammatory cytokines<sup>53</sup> (Fig. 3C). Jeong *et al.* further developed this technology by creating a seven-channel device for studying the effects of tumor spheroids on fibroblast activity (Fig. 3D).<sup>54</sup>

The examples described above represent a common methodology for including cell-laden hydrogels in existing microfluidic devices, where the prepolymer of the gel is delivered to fill a channel or chamber *via* capillary action and is held in place by surface tension. After subsequent curing media is perfused through an adjacent channel, which contacts one side of the gel structure, for nutrients and oxygen to be transported to the cells therein through diffusion. While simple and straightforward, this method has challenges in specific applications. First, it suspends cells in a gel without considering cell alignments. Many cell types such as skeletal muscle fibers need to be aligned to exert normal functions.<sup>55</sup> Second, the lateral flow of media along the surface of a gel and the diffusion mechanism for supplying nutrients and removal of waste may be limited in terms of efficiency—evidence shows that a gel thicker than 200 μm can cause cell necrosis due to insufficient oxygen delivery.<sup>56</sup> To circumvent these issues, precise gel localization using photolithography has been developed.

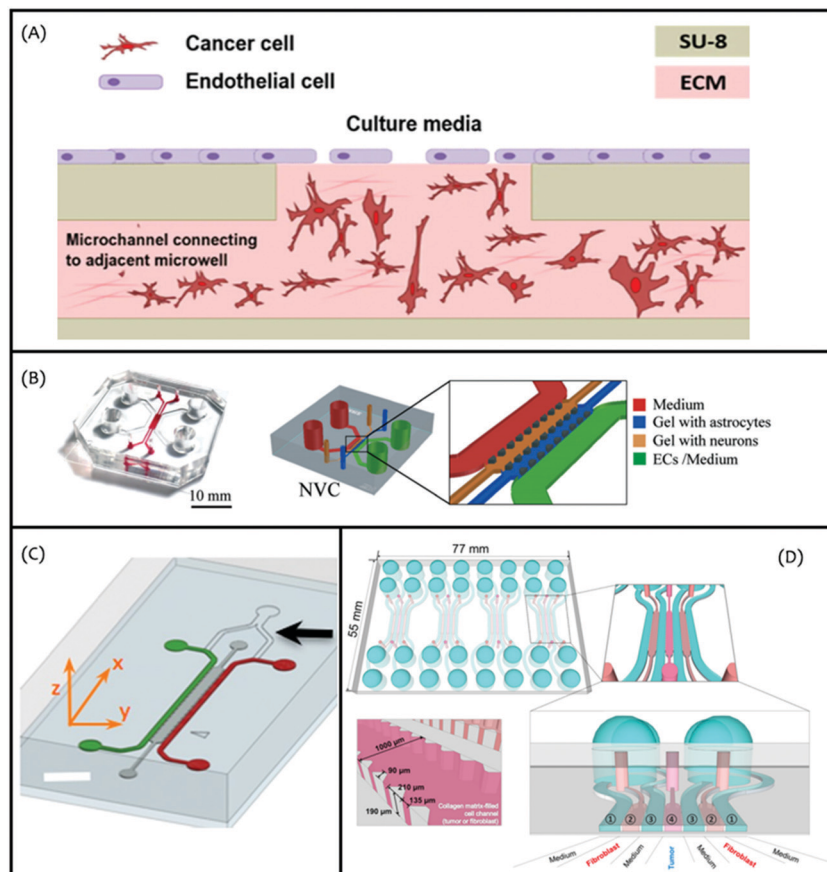


**Fig. 3** Recent examples of integrating cell-laden hydrogels in premade microfluidic devices. (A) Schematic of the device developed by Virumbrales-Munoz *et al.* Tumor cells were cultured in a collagen matrix (pink) with a monolayer of endothelial cells cultured on top to create a permeable barrier. Reprinted from Virumbrales-Munoz (2017) with permission. (B) A four-channel microfluidic device where the two inner channels were filled with hydrogels containing astrocytes and neurons, respectively. The outer channels delivered medium to nourish the cells. Reprinted from Adriani *et al.* (2017) with permission. (C) A microfluidic device with two fluid channels (green, red) and a central channel containing hydrogel (grey). TCR-T cells flowing through the red channel diffused into the central hydrogel channel and attacked hepatocytes within. Reprinted from Zervantonakis *et al.* (2012) with permission. (D) Illustration of a seven-channel device with four flow channels (1, 3) flowing media through and three channels containing hydrogels (2, 4). Contact with the fluid channels was allowed by small gaps in the channel walls as seen in bottom left. Reprinted from Jeong *et al.* (2016) with permission.

For example, Agrawal *et al.* demonstrated an innovative muscle-on-a-chip model using a photomask to specifically form two hydrogel pillars (100–300  $\mu\text{m}$ ) within a microfluidic channel. Next, GelMA containing C2C12 muscle cells was cured in a capsule shape between the pillars using a second photomask. The results showed that the micropillars acted as anchoring points to force the cells to form uniaxially-aligned, densely-packed 3D muscle cylinders.<sup>57</sup> Skardal *et al.* recently created a liver-on-a-chip model with enhanced molecular diffusion through hydrogel. A photomask was applied to form islets of cell-laden hydrogels within flow paths, such that media could flow around the islets and molecules diffusing from all sides of the gel structure.<sup>58</sup> With this design, liver cells (HEPG2) were alive and functional for over seven days.<sup>58</sup> Overall, photolithography-assisted hydrogel inclusion in microfluidic devices provides precise localization and patterning of cells. However, it usually requires UV light to cure the gels which may cause phototoxicity issues. All these factors should be considered when choosing a method for organs-on-a-chip research.

### Fabrication of microchannels in hydrogel parts

**Replica molding.** Replica molding can be used to make microfluidics in hydrogels without photocuring limitations. There are three types of molds that are commonly used to cast hydrogel-based microfluidic devices: master molds prepared by photolithography, physically removable molds, and sacrificial molds. As shown in Fig. 4A, a master can be prepared by allowing irradiation to pass through the transparent pattern on the photomask, which cross-links the photoresist material (*e.g.* SU-8) in place, creating a raised serpentine microstructure (Fig. 4B). Next, the prepolymer of a hydrogel is poured onto the mold (Fig. 4C) followed by gelation. After the hydrogel slab is peeled off, it can be sealed to a substrate such as glass to close the channel for flow-based experiments (Fig. 4D). For example, Cabodi *et al.* utilized this technology to fabricate a microfluidic device by casting an alginate solution on top of a patterned photoresist prepared *via* lithography.<sup>59</sup> The cross-sections of microchannels fabricated by this method are typically rectangular, but research into scaffold geometry indicates that cell adhesion is affected by the shape of

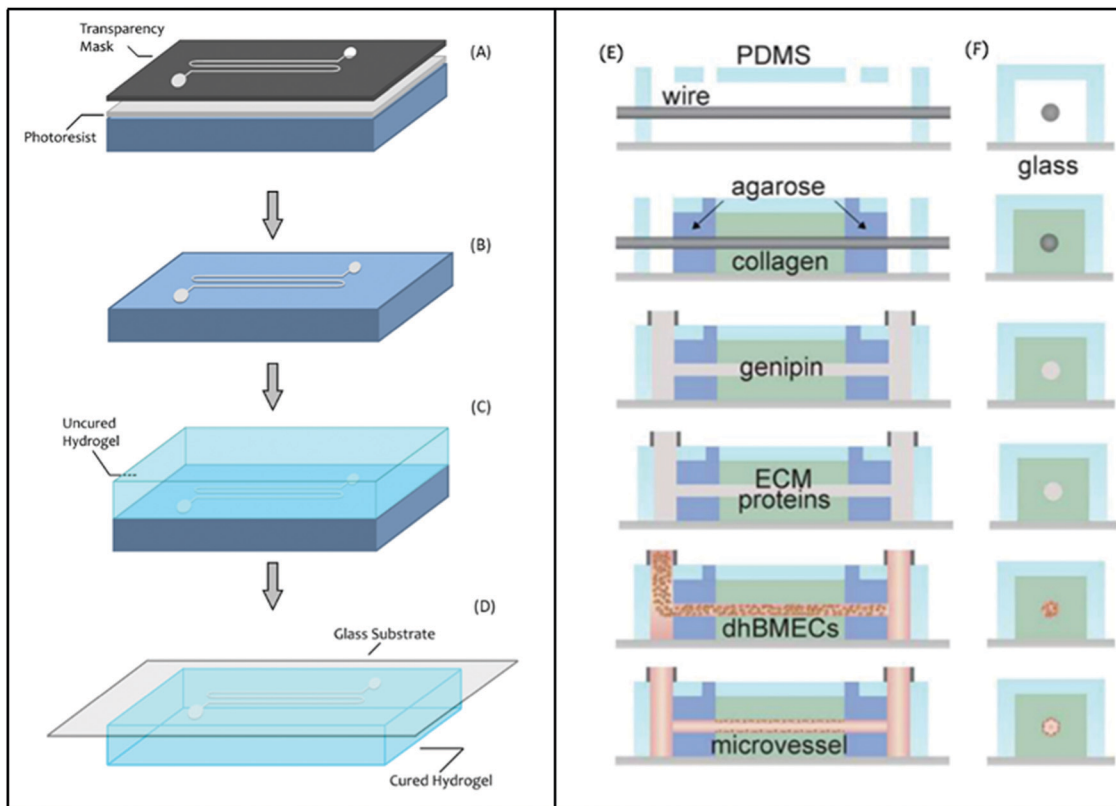


**Fig. 4** Using molds to make microfluidic channels in hydrogels. (A) Applying a mask on top of a photoresist (SU-8) layer so that only the exposed region is crosslinked. (B) Removing the uncured photoresist to have raised microstructures. (C) A hydrogel is cast on top of the mold, cross-linked, and an imprint of the microstructure is left in the casting material. (D) A substrate, often glass, is pressed onto the cast hydrogel to seal the channel. (E and F) Fabrication of microchannels using a wire mold (150  $\mu\text{m}$  diameter). Collagen and agarose were gelled around the suspended wire; when the wire was removed a channel is left in the hydrogel which was seeded with differentiated human brain microvascular endothelial cells (dhBMECs). Reprinted with permission from Linville *et al.* (2019).

the substrate, where rectangular (cross section) channels show a lower degree of cell adhesion.<sup>60</sup> Therefore, He *et al.* developed a more complicated methodology for fabricating hydrogels with circular channels to better emulate internal vasculature. This was accomplished by partially crosslinking gelatin which was cast on a semi-circle mold, aligning it with another gelatin cast, and completing the crosslinking to form circular hollow channels.<sup>61</sup> The way that a closed microfluidic channel is formed (binding a hydrogel layer on a substrate) can be challenging in subsequent applications. Due to the flexibility of hydrogels, deformation will likely occur when placing a gel layer on a substrate (*e.g.*, stretching), which can compromise the dimensions and shapes of the desired microstructures. Using less flexible hydrogels and alignment markers can be a potential solution to this issue.<sup>62</sup> Some groups measured the amount of shrinkage that occurred under different conditions and adjusted the mold pre-emptively for curing results in the desired final dimensions.<sup>63</sup>

Existing microstructures such as micron-diameter wires can also be embedded in hydrogels to form microchannels. For example, Linville and Wong prepared hollow microfluidic channels in hydrogel-based devices by crosslinking polymers such as collagen and agarose around a wire which was pulled out after the hydrogel gelled<sup>64,65</sup> (Fig. 4E and F). It is simple

and straightforward to fabricate devices using such physically removable molds. However, this method can only generate devices with basic and simple microstructures (*e.g.* straight channels).

Sacrificial molds can be used to fabricate complicated hollow microstructures in a piece of hydrogel. These molds are made by certain materials such as gelatin,<sup>66</sup> PVA (polyvinyl alcohol),<sup>67</sup> and alginate<sup>68</sup> which can be dissolved after the surrounding hydrogel is fully cured. A recent example is by Tocchio *et al.*; a mold was etched in plexiglass, PVA was carefully poured into it, dried overnight, and removed<sup>67</sup> (Fig. 5A). This mold was then placed between glass spacers and covered in either 2-hydroxyethyl methacrylate (HEMA), agarose, or GelMA.<sup>67</sup> Following curation of the hydrogels and removal of the spacers, the PVA was dissolved by washing with water or phosphate-buffered saline<sup>67</sup> to form hollow channels in the hydrogel (Fig. 5B) which could be seeded with endothelial cells to mimic a vasculature system (Fig. 5C). Sacrificial molds provide a low-cost way to fabricate desired microstructures in hydrogel. However, certain concerns may arise from the additional washing step: the buffer composition may cause chemical contamination and/or osmotic shock to the cells; maintaining sterilization may also be difficult.

Overall, replica molding is a simple technique to fabricate hydrogel microfluidic devices, however, limitations and

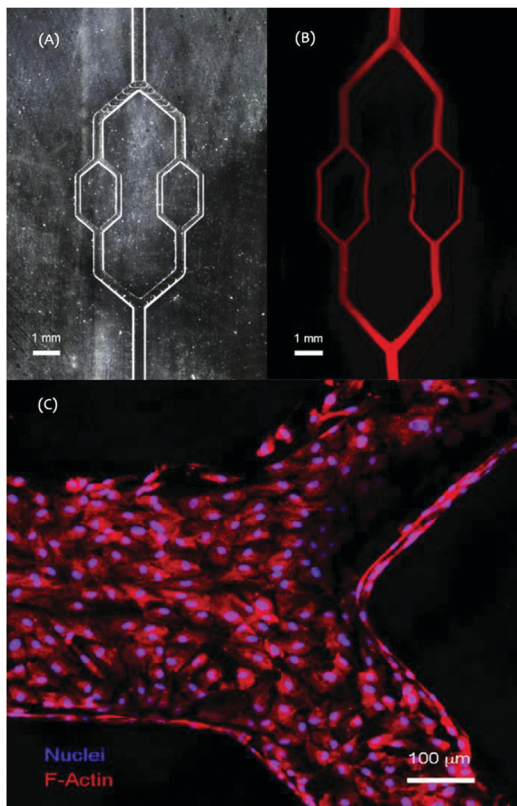


Fig. 5 Using a sacrificial mold to make microfluidic channels in hydrogel. (A) Image of the sacrificial mold made from PVA using an etched glass patterner. (B) After the PVA mold was removed from the cured hydrogel around it, hollow channels were formed. The image shows fluorescent microspheres flowing through the channels. (C) An immunofluorescent image of HUVECs seeded on the inside of the channels as blood vessel mimics. Reprinted from Tocchio *et al.* (2015) with permission.

challenges exist. To maintain the structural integrity of such a device, relatively stiff materials are commonly used which may not support viable cell encapsulation due to the high material density (*e.g.* limited number and size of the pores for diffusion). This perhaps explains why these studies mainly used the inner wall of the microchannels as a support surface to seed endothelial cells as a vasculature mimic. In addition to the deformation issue of microstructures in a soft gel, ports at the ends of flow channels to connect tubing and adaptors for liquid delivery/perfusion can also be challenging. The most frequently used method for creating ports is using punchers, which excise a portion of the hydrogel of the punch's diameter. Currently, the success of this method relies on user expertise both for using punchers and appropriately curing the hydrogel device, and the flexible gel may not be able to seal a tubing tightly for leakage-free flows. To circumvent these issues, efforts will be needed for new device designs and fabrications. For instance, the device shown in Fig. 4E was not connected to tubing. Instead, the device was placed vertically with a reservoir on top filled with media, and gravity drove the flow through the channel. Multiple materials can also be used to fabricate such a device, with gels of high mechanical strengths in the port area for reliable port punching.

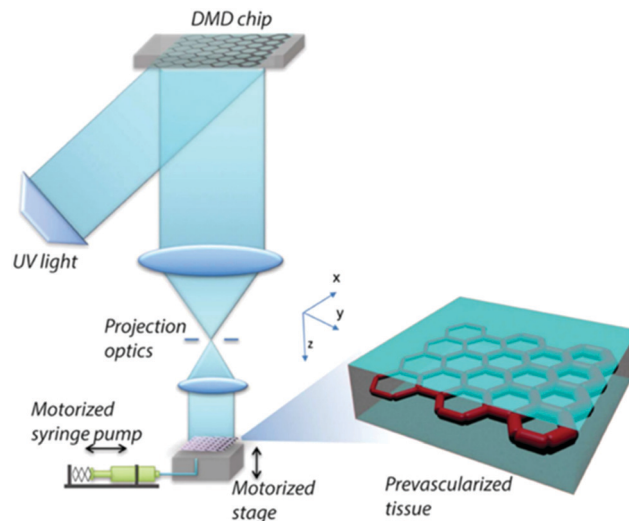
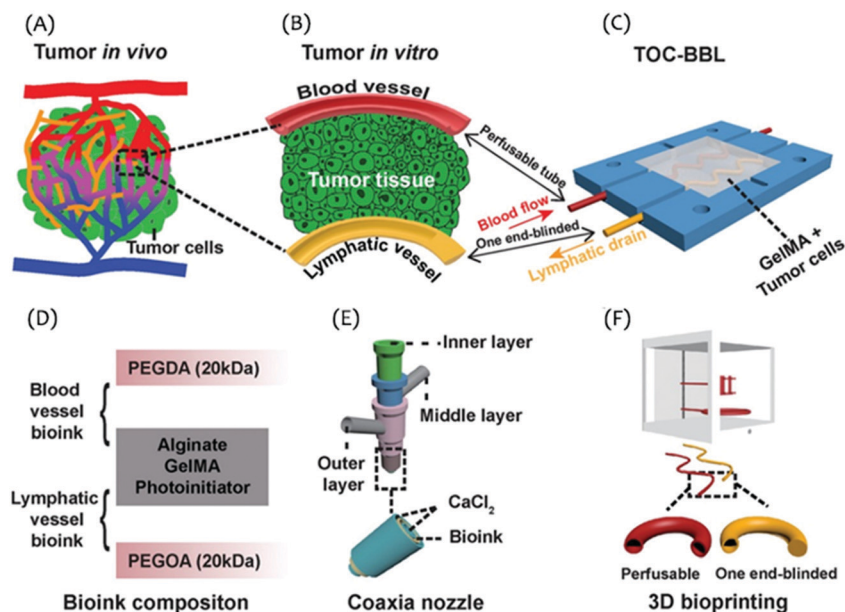


Fig. 6 Schematic of bottom-up 3D printing with optical curing. A thin layer of prepolymer is loaded onto the motorized stage and the optics are used to select regions for crosslinking. Unpolymerized material is washed off, the stage lowered, and additional layers are loaded on top and crosslinked to build a 3D device. Reprinted from Zhu *et al.* (2017) with permission.

**3D bioprinting.** Extrusion-based bioprinting has gained interest in recent years for creating tissue models due to its capability for fabricating 3D structures with desired dimensions and shapes in one step.<sup>69</sup> A typical 3D bioprinting process is to extrude bioinks (*e.g.* hydrogel prepolymer with suspended cells) onto a stage layer by layer.<sup>69</sup> Each layer is cured *via* various mechanisms such as photo irradiation and chemical crosslinkers. Fig. 6 illustrates how a 3D bioprinter works with optical components to cure the gel. Numerous bioprinted tissue models have been reported. For example, Cao *et al.* directly printed a mixture of either PEGDA or poly(ethylene glycol) octaacrylate (PEGOA) with GelMA, alginate, and photoinitiator to form microfluidic tubes<sup>70</sup> (Fig. 7). These printed tubes acted as blood and lymphatic vessel mimics which were then sealed within a GelMA matrix containing suspended MCF-7 tumor cells. Therefore, a tumor model that contained blood flow, lymphatic drainage, and cancer cells embedded in surrounding hydrogels was fabricated.<sup>70</sup>

To avoid the cytotoxicity issue of common photoinitiators, Grigoryan *et al.* recently reported that biocompatible food color molecules can be used to cure PEGDA hydrogels.<sup>71</sup> They also developed a home-made digital micro-mirror setup for the fabrication of complicated microchannel networks. They first manufactured an acellular interconnected channel network to study the oxygenation of red blood cells (Fig. 8), which was achieved by using a 20% (w/w) by weight PEGDA (6 kDa) solution, as this gel was determined to allow for oxygen diffusion and relatively long-term mechanical stability (device could withstand 10 000 ventilation cycles). Although not stated by the authors, it is likely that the PEGDA hydrogel may be too dense to encapsulate cells for direct tissue printing, because in a subsequent experiment, the authors fabricated a PEGDA holder with a prefill space, where fibroin or GelMA gels with suspended hepatocyte aggregates were filled and cured *in situ*.



**Fig. 7** 3D bioprinting to mimic tumor microenvironments. (A) *In vivo* depiction of a tumor microenvironment. (B) Simplified view of the *in vitro* microenvironment for studying tumor cells. (C) Image of the proposed device for studying tumor cells where the blood vessel (red) carried media through the device and out the other side and the one-sided lymphatic channel (yellow) to enable drainage. (D) Bioink composition for blood vessel fabrication (top, middle) and lymphatic vessel fabrication (middle, bottom). (E) The setup of the bioprinting extrusion nozzle, illustrating the codelivery of both the bioink and crosslinking agent ( $\text{CaCl}_2$ ). (F) Example bioprinting of the blood vessel and lymphatic vessels to be used in the final device. Reprinted from Cao *et al.* (2019) with permission.

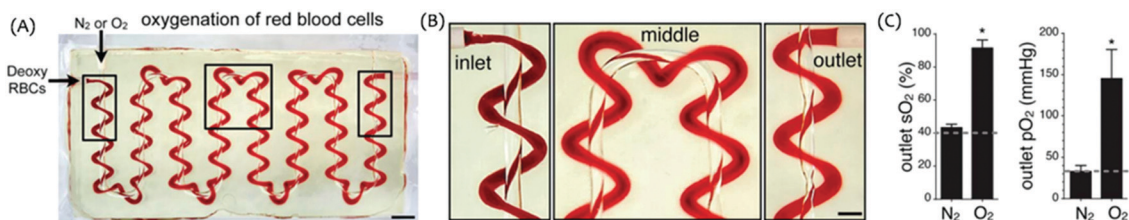


**Fig. 8** A microfluidic blood vessel mimic directly fabricated in poly(ethylene glycol) diacrylate (PEGDA) hydrogel via stereolithography. (A) Top-down view of the PEGDA hydrogel with interwoven oxygen (clear) and RBC (red) delivery channels. (B) A zoomed-in view of the channels. The color change from dark red to a lighter red by the time RBCs reach the end of the channel indicated efficient oxygen exchange between the gas and the blood channels. (C) Quantitated gas exchange efficiency on the device. Reprinted from Grigoryan *et al.* (2019) with permission.

Recreating an accurate *in vivo* mimic often requires the use of multiple materials to simulate the different parts of an organ/tissue;<sup>72</sup> fabrication of such systems can be carried out by 3D bioprinting. For example, Ruiz-Cantu *et al.* produced a neocartilage model using chondrocyte-laden GelMA co-printed with polycaprolactone (PCL).<sup>72</sup> Kang *et al.* bioprinted a fine-tuned mixture of gelatin, fibrinogen, hyaluronic acid, and glycerol prepared in Dulbecco's Modified Eagle Medium (DMEM) to make ear constructs.<sup>73</sup> These constructs were implanted in mice and were observed to retain structural integrity over two months and showed signs of surface vascularization.<sup>73</sup> Arumugasamy *et al.* recently reviewed multimaterial bioprinting and its applications at length.<sup>74</sup>

The historical drawback of 3D bioprinting is the low resolution due to the flexibility of the bioinks and the relatively slow kinetics for curing the hydrogel matrix.<sup>75</sup> However, recent advances have lowered the achievable resolution making it a more attractive

option.<sup>76–78</sup> An example of such is light-assisted printing where the resolution is dependent on the light source rather than the printing head of an extruder.<sup>69</sup> Light-assisted techniques have their own drawbacks, such as potential cytotoxicity and limitations in printing materials, but are able to push printing resolutions down to 5  $\mu\text{m}$  or lower whereas extrusion-based methods are currently limited to 100  $\mu\text{m}$  and higher.<sup>69</sup> Another concern of 3D bioprinting is the high shear stress expressed to the cells. When a stream of bioink with cells is pushed out of the extruder orifice, the cells are experiencing a high level of shear, which may be deleterious for the cells.<sup>79</sup> This is especially true when applying a smaller orifice to improve resolution.<sup>79</sup>

Like the replica molding technology, 3D-bioprinting also makes microfluidic devices from hydrogels—a stiff and dense gel can maintain the structural integrity but compromise cell viability therein. In an analysis of recent publications, the reported bioprinted devices can be grouped into two categories:



those with cells encapsulated to mimic a tissue *in vivo*, and others that act merely as a support structure for subsequent cell seeding or perfusion (*e.g.* erythrocytes perfused through a device to mimic blood flow, the example in Fig. 8). In the case of the former, it is exceedingly important that the hydrogel chemistry and physics can mimic the *in vivo* environment. Specifically, the bioink used during 3D printing must provide cell adhesion moieties, be permeable for oxygen and small molecules, and be mechanically stable.<sup>80,81</sup> Common naturally occurring materials used as bioinks are those based on agarose, alginate, collagen, and hyaluronic acid.<sup>80</sup> Agarose dissolves and is handled easily, gels at low temperatures, and maintains dimensionality for long periods of time.<sup>81</sup> However, low cell adhesion and proliferation as well as limited biosynthesis of cell components has indicated that agarose on its own is insufficient for cell culturing.<sup>82,83</sup> Kreimendahl *et al.* demonstrated the feasibility of blending agarose with collagen and fibrinogen to promote cell culturing while maintaining structural stability.<sup>84</sup> Alginate is a commonly used material owing to its abundance, low cost, and characterized diffusion properties.<sup>85</sup> Furthermore, alginate can be cured significantly quicker than thermally-cured hydrogels through the use of multivalent cations.<sup>85</sup> However, monolithic alginate hydrogels lack mechanical stability and adhesion sites, limiting cell attachment.<sup>81</sup> Strategies to overcome these shortcomings have been demonstrated; Jia *et al.* developed a mixture of alginate, GelMA, and PEG-tetra-acrylate (PEGTA) to form a high-strength device with perfusable vasculature.<sup>86</sup> Functionalization of alginate channels with specific peptides has also been demonstrated to promote cell adhesion.<sup>87</sup> Although collagen is commonly used for cell culturing, it is difficult to be used for 3D bioprinting due to its long cure times, during which homogeneity of cell distribution may be lost as cells spread.<sup>81</sup> Modified collagens have made it a viable bioprinting material. For instance, Homenick *et al.* demonstrated this by crosslinking collagen with poloxamers to increase the Young's modulus of the overall material.<sup>81</sup> Overall, as natural materials have low tunability of their mechanical properties, it is simpler to blend them with synthetics which can have various properties (*e.g.* molecular weight, degree of functionality, types of functional groups) adjusted based on the needs of the application.<sup>80</sup>

When hydrogels are used as a microfluidic device material to support subsequent cell inclusion, maintaining mechanical stability becomes a necessity along with other considerations such as non-specific molecular adsorption/absorption and surface tensions.<sup>88</sup> Protocols have been reported to functionalize parts of such as device for specific cell applications. For example, Koh *et al.* formed microwells for the isolated culturing of cells by fabricating a layer of PEG hydrogel walls which circumscribed a hydrophobic floor to selectively pattern cells.<sup>89</sup> A similar approach was shown by Lee *et al.* where micropatterned PEG hydrogels, acting as walls/dividers, were placed over a network of electrospun fibers for the localization of cells.<sup>90</sup>

In conclusion, with current technologies, it is critical to choose a proper material for 3D-bioprinting. In addition to the chemistry of a material, the curing conditions (*e.g.* temperature, time, radiation, *etc.*) can also affect the crosslink density,

porosity, and mechanical properties, which need to be optimized for each specific application.

## Electrospun fibers as scaffolding materials for organs-on-a-chip

### An overview of electrospinning

**The technology of electrospinning.** Electrospinning is a technique that utilizes a high electrical voltage to generate polymer fibers on the micro- and nanometer scale.<sup>91</sup> As shown in Fig. 9, a typical electrospinning setup consists of a syringe for dispensing a polymer solution through a metal needle. A high voltage (in the range of 5–30 kV) is applied to the metal needle, where a Taylor cone forms.<sup>92</sup> The fibers are electrically charged and thus can be deposited on a grounded collector. Due to the tuneable fiber diameter and mechanical stiffness, and the ability to embed particles/compounds, electrospun fibers have been utilized in various applications as scaffolding materials for 3D cell culture.<sup>93–96</sup>

**Commonly used polymers in electrospinning.** Both synthetic and natural polymers have been implemented in electrospinning; some of the most commonly used ones are summarized in Table 2. After a literature search *via* Web of Science using keywords “Electrospinning” and “Extracellular Matrix”, it was determined that PCL (polycaprolactone) and PLA (polylactic acid) are the two most common materials due to their biocompatibility and biodegradable nature.<sup>97–100</sup> Fig. 10A shows the popularity of common materials for electrospinning.<sup>101–195</sup> Most of the research implementing electrospinning focuses on biomimetic tissue engineering such as 3D cell cultures (Fig. 10B).

In addition to synthesized polymers, the use of natural polymers for electrospinning was also explored. For example,

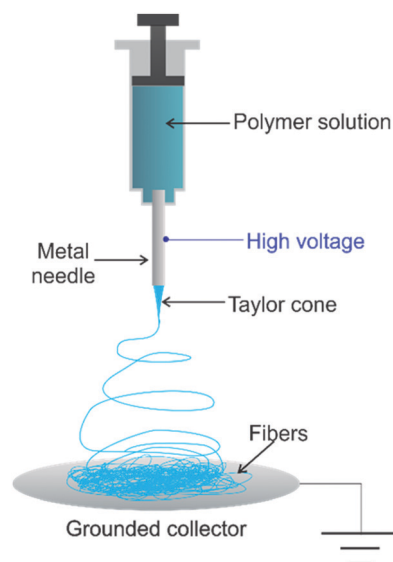
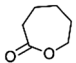
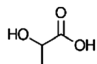
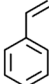
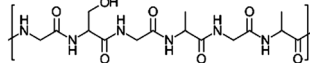
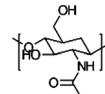
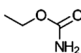
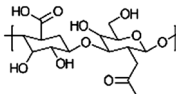


Fig. 9 The electrospinning setup. A polymer solution is pushed through a metal needle where a high voltage is applied. A Taylor cone erupts at the end of the needle tip and fibers are formed. The fibers can be collected on a grounded surface.

Table 2 Common electrospinning polymers and properties

| Name of polymer                 | Abbreviation | Biodegradable (Y/N) | Biocompatible (Y/N) | Natural/synthesized | Structure (monomer)                                                                 |
|---------------------------------|--------------|---------------------|---------------------|---------------------|-------------------------------------------------------------------------------------|
| Poly( $\epsilon$ -caprolactone) | PCL          | Y                   | Y                   | Synthesized         |  |
| Collagen                        | N/A          | Y                   | Y                   | Natural             | N/A                                                                                 |
| Poly(lactic acid)               | PLA          | Y                   | Y                   | Synthesized         |  |
| Fibronectin                     | N/A          | Y                   | Y                   | Natural             | N/A                                                                                 |
| Poly(styrene)                   | PS           | N                   | Y                   | Synthesized         |  |
| Silk fibroin                    | N/A          | Y                   | Y                   | Natural             |  |
| Chitosan                        | N/A          | Y                   | Y                   | Natural             |  |
| Polyurethane                    | PU           | N                   | Y                   | Synthesized         |  |
| Hyaluronic acid                 | HA           | Y                   | Y                   | Natural             |  |

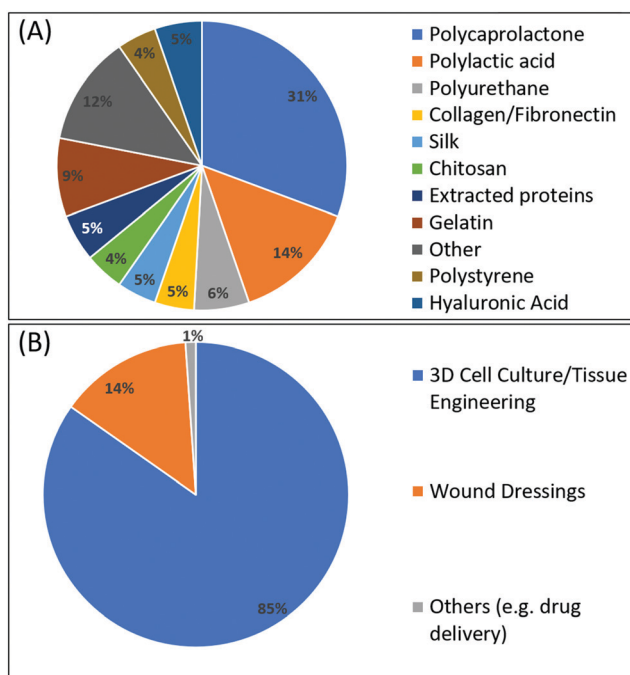


Fig. 10 Results of our literature survey regarding electrospinning materials and applications. (A) PCL (polycaprolactone) and PLA (poly(lactic acid)) are the most common polymers used in electrospinning. (B) The main applications of electrospinning are tissue engineering, 3D cell culture, and wound dressing.

collagen and fibronectin solutions can be directly electrospun to generate more physiologically relevant ECMs than synthetic polymers.<sup>196</sup> Silk fibroin has been gaining attention recently

due to its remarkable characteristics including biocompatibility, high water and oxygen uptake, and tunable mechanical properties.<sup>197</sup> This material can be extracted from raw silk following a simple protocol at low costs.<sup>198</sup>

### Integration of electrospun fibers in microfluidics for organs-on-a-chip studies

Most of the applications of electrospun fibers have used static containers to culture cells. A standard protocol is to peel the electrospun fiber layer off from the collector, cut it to the desired shape, and then place it in a multi-well plate for cell seeding after sterilization.<sup>199</sup> Although simple, this protocol excludes the potential benefits of flow-based cell cultures such as shear stress introduction, continuous nutrient supply and waste removal, and gradient control. Therefore, since 2016, efforts have been made to combine electrospun fibers as scaffolding materials in microfluidics to prototype organs-on-a-chip models. There are three main technologies developed for this purpose: lateral-flow models, direct electrospinning of fibers into a microfluidic channel, and modular integration of electrospun fibers.

**Lateral-flow model.** Pimentel *et al.* recently developed a microfluidic device on a sheet of electrospun fibers (poly(L-lactic acid), PLLA) as a lateral-flow model for cell culture.<sup>200</sup> As shown in Fig. 11A, certain areas on a sheet of electrospun fibers (the whole square) were blocked to form hydrophobic barriers (black; blocking material was not specified by the authors) surrounding channels and circular zones. Like paper-based microfluidics, the fibrous nature of the substrate can drive liquid flow *via* capillary actions. However, compared to paper, electrospinning offers the possibility to make fibers of desired dimensions and morphologies (Fig. 11B) for specific cell culture applications.

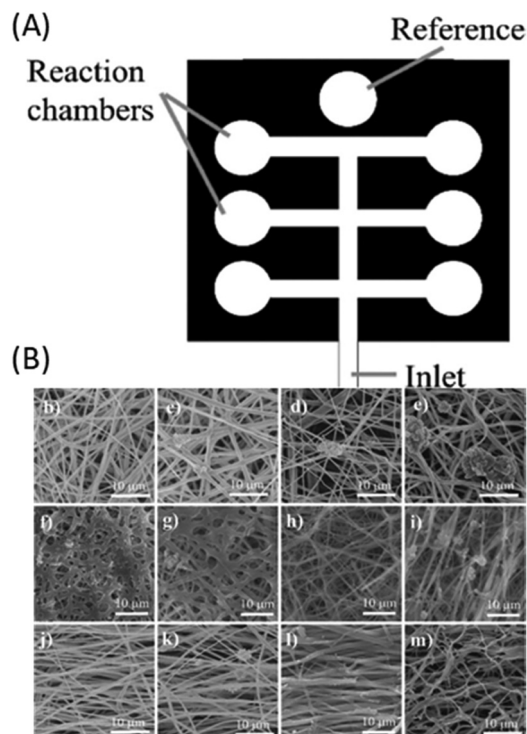


**Fig. 11** (A) The layout of the lateral-flow device created by Pimentel *et al.* On a piece of electrospun fibers, certain areas are blocked (black) with the rest defined as channels and chambers, where liquid can be delivered via capillary actions. (B) Electrospun fibers with various microstructures were tested for cell culture. Reprinted from Pimentel *et al.* (2020) with permission.

Also, other components can be premixed in the polymer solution to make composite fibers. For example, the authors added NaY, a crystal sodium zeolite, to the fiber to increase the hydrophilicity of the material.<sup>178</sup>

This technology has unique advantages including simple fabrication and assay parallelization (multiple chambers in one device). However, such devices are not suitable for cell types that require flow-based shear stress.

**Direct electrospinning of fibers into a microfluidic channel.** Chen *et al.* invented a technology in 2016 called dynamic focusing electrospinning, to directly coat electrospun fibers on the inner side of a fluidic channel.<sup>201</sup> As demonstrated in Fig. 12A, a 3D-printed sheath device was placed around the metal needle/cannula. With proper pressure, the gas (air or N<sub>2</sub>) flowing out of the sheath confined the PCL fibers through the fluidic channel placed under the Taylor cone. The exiting fibers from the bottom end of the fluidic device indicated successful fiber coating inside the channel. A uniform layer of microfibers was added to the channel wall, which was confirmed by SEM imaging (Fig. 12B). The authors cultured RAW 264.7 macrophages and found that the fibrous scaffold enhanced the production of cytokines such as interleukin-6 (IL-6) and vascular endothelial growth factor (VEGF).

This technology can introduce the flow through a 3D tissue mimic. However, a limitation is that the diameter of the fluidic channel cannot be smaller than 1 mm. Although the fibers can

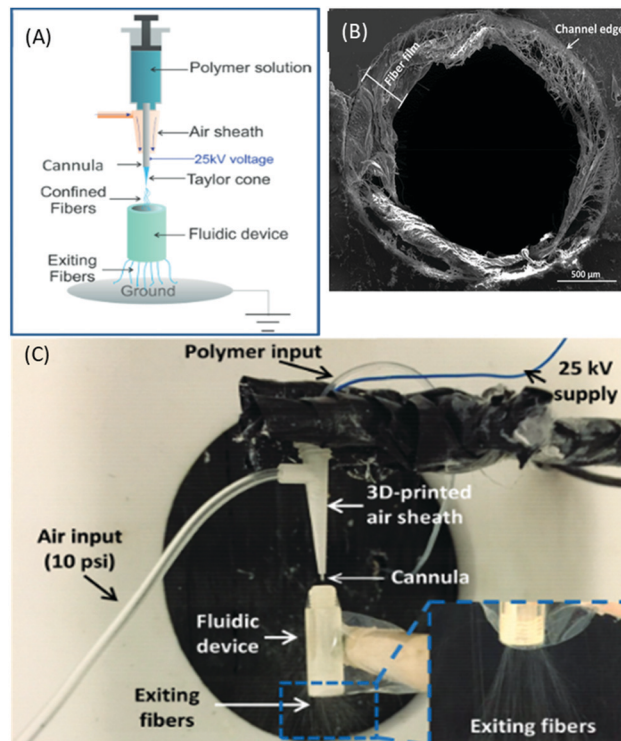


**Fig. 12** Using dynamic focusing to confine microfibers into a fluidic device. (A) The electrospinning setup with air sheath to focus the fibers into a fluidic channel. (B) An SEM image of the cross-section of a device showing a layer of electrospun fibers was deposited on the inside of the channel. (C) The real picture of the setup. Fibers exiting from the other end of the fluidic device (inset) suggest successful fiber focusing. Reprinted from Chen *et al.* (2016) with permission.

be focused by the sheath flow, there is a limit of the focusing because the fibers tend to spread due to the same charges they bear. Also, the pressure of the gas flow cannot be too high, or disruption of the Taylor cone will occur.

**Modular integration of electrospun fibers in microfluidic devices.** Chen *et al.* reported another technology to modularly integrate fibers in microfluidics in 2018.<sup>202</sup> As shown in Fig. 13A, instead of directly electrospinning into a microfluidic channel, the fibers were coated on a polystyrene sheet first, which was then laser cut into rectangular inserts.<sup>203</sup> The fused edges by the laser immobilized the fibers on the PS substrate. After cells were seeded on the fibers, the inserts were plugged into a 3D-printed fluidic device with matching slots (Fig. 13B). The space between the inserts form the fluidic channel for media to flow through (Fig. 13C and D). The authors demonstrated that under lipopolysaccharide (LPS) stimulation, the response rates of macrophages cultured in the fibrous scaffolds are more physiologically relevant than those cultured on a flat surface.

This technology has prominent advantages. Modularity allows for examination of the cells cultured on the inserts before assembly, with failed cultures (*e.g.* by contamination) being replaced without discarding the whole setup. After an experiment, the cell-laden inserts can be removed for further studies

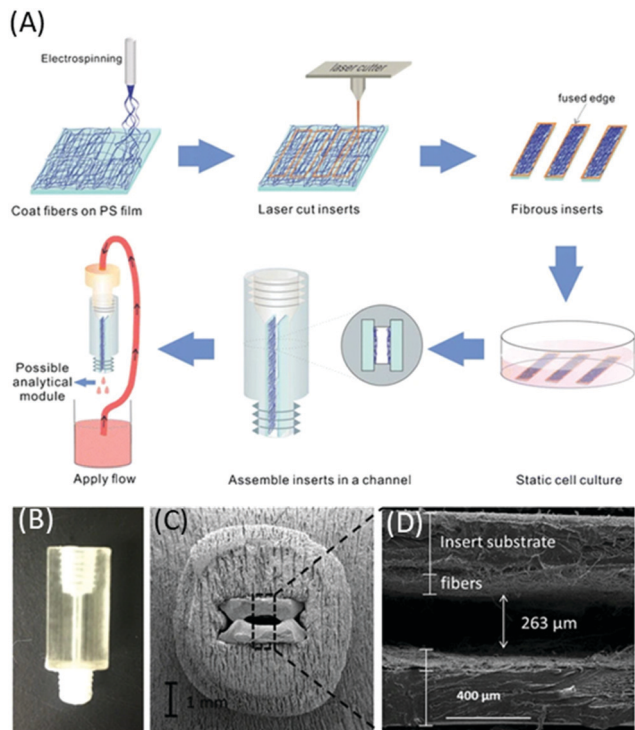


**Fig. 13** Insert-based microfiber integration in microfluidic devices. (A) The workflow of the technology. Electrospun fibers were first coated on a PS film, which was laser cut into rectangular inserts of desired dimensions. After cells were seeded in on the fibers, the inserts were integrated into 3D-printed fluidic devices with matching slots for flow-based stimulation and downstream quantitation. (B) The 3D printed fluidic device. (C) A cross view of an assembled device. The two cell-laden inserts fit the slots precisely with the distance in the middle forming the fluidic channel. (D) A zoomed-in view of the inserts. The fiber layers could be seen. Reprinted from Chen *et al.* (2018) with permission.

such as imaging. The space between inserts is customizable for tuning shear stress. In our opinion, this is the most applicable technology for integrating electrospun fibers in microfluidics to date.

## Conclusion and perspective

In this paper, we thoroughly reviewed recent (mainly after 2016) advances in integrating scaffolding materials in microfluidics for organs-on-a-chip applications. Various technologies have been developed to incorporate hydrogel materials and electrospun fibers on chips for disease modeling, pathophysiological studies, and pharmaceutical research, with insightful results generated. After reviewing these models, we found that they were fabricated by complicated protocols *via* high-end/expensive instruments, which may explain why the technologies have not been widely translated. Organs-on-a-chip hold the potential for extensive breakthroughs in disease modeling, drug discovery, and enhancing our understanding of organ functions. However, this promising potential will not be achieved without easy translation of the technology to other laboratories (*e.g.* those with expertise in physiology but not chip fabrication). Simplified and translational

devices should be a research focus in the future. Modularity can help technology translation; compared to all-in-one devices which must be discarded if any part fails, modular microfluidic devices are more cost-efficient and flexible. For example, a toolkit with various modules can be developed, with which organs-on-a-chip models can be simply assembled based on specific needs. Also, protocols need to be standardized. For instance, to cure collagen hydrogel at 37 °C, different curing times have been reported. Standardizing such protocols will benefit technology translation. Lastly, most of the reported organs-on-a-chip models were single-use devices with only one throughput. Considering the high labor, time, and facility investments to the fabrication, these factors can depress enthusiasm. Therefore, reusable devices with enhanced throughput need to be exploited.

## Conflicts of interest

There are no conflicts to declare.

## References

- 1 J. A. DiMasi, H. G. Grabowski and R. W. Hansen, Innovation in the pharmaceutical industry: New estimates of R&D costs, *J. Health Econ.*, 2016, **47**, 20–33.
- 2 B. Y. Zhang and M. Radisic, Organ-on-a-chip devices advance to market, *Lab Chip*, 2017, **17**(14), 2395–2420.
- 3 A. Ghanemi, Cell cultures in drug development: Applications, challenges and limitations, *Saudi Pharm. J.*, 2015, **23**(4), 453–454.
- 4 M. Tyers and M. Mann, From genomics to proteomics, *Nature*, 2003, **422**(6928), 193–197.
- 5 C. M. Sakolish, M. B. Esch, J. J. Hickman, M. L. Shuler and G. J. Mahler, Modeling Barrier Tissues In Vitro: Methods, Achievements, and Challenges, *EBioMedicine*, 2016, **5**, 30–39.
- 6 M. H. Wu, S. B. Huang and G. B. Lee, Microfluidic cell culture systems for drug research, *Lab Chip*, 2010, **10**(8), 939–956.
- 7 G. M. Whitesides, The origins and the future of microfluidics, *Nature*, 2006, **442**(7101), 368–373.
- 8 A. Polini, L. Prodanov, N. S. Bhise, V. Manoharan, M. R. Dokmeci and A. Khademhosseini, Organs-on-a-chip: a new tool for drug discovery, *Expert Opin. Drug Discovery*, 2014, **9**(4), 335–352.
- 9 K. Ronaldson-Bouchard and G. Vunjak-Novakovic, Organs-on-a-Chip: A Fast Track for Engineered Human Tissues in Drug Development, *Cell Stem Cell*, 2018, **22**(3), 310–324.
- 10 S. Ishida, Organs-on-a-chip: Current applications and consideration points for in vitro ADME-Tox studies, *Drug Metab. Pharmacokinet.*, 2018, **33**(1), 49–54.
- 11 R. C. Dutta and A. K. Dutta, Cell-interactive 3D-scaffold; advances and applications, *Biotechnol. Adv.*, 2009, **27**(4), 334–339.
- 12 M. J. Bissell, D. C. Radisky, A. Rizki, V. M. Weaver and O. W. Petersen, The organizing principle: microenvironmental

- influences in the normal and malignant breast, *Differentiation*, 2002, **70**(9–10), 537–546.
- 13 K. Chitcholtan, P. H. Sykes and J. J. Evans, The resistance of intracellular mediators to doxorubicin and cisplatin are distinct in 3D and 2D endometrial cancer, *J. Transl. Med.*, 2012, **10**, 38.
  - 14 K. M. Hakkinen, J. S. Harunaga, A. D. Doyle and K. M. Yamada, Direct comparisons of the morphology, migration, cell adhesions, and actin cytoskeleton of fibroblasts in four different three-dimensional extracellular matrices, *Tissue Eng., Part A*, 2011, **17**(5–6), 713–724.
  - 15 D. Kloss, R. Kurz, H. G. Jahnke, M. Fischer, A. Rothermel, U. Anderegg, J. C. Simon and A. A. Robitzki, Microcavity array (MCA)-based biosensor chip for functional drug screening of 3D tissue models, *Biosens. Bioelectron.*, 2008, **23**(10), 1473–1480.
  - 16 P. A. Janmey, D. A. Fletcher and C. A. Reinhart-King, Stiffness Sensing by Cells, *Physiol. Rev.*, 2019, **100**(2), 695–724.
  - 17 F. Pampaloni, E. G. Reynaud and E. H. Stelzer, The third dimension bridges the gap between cell culture and live tissue, *Nat. Rev. Mol. Cell Biol.*, 2007, **8**(10), 839–845.
  - 18 C. Jensen and Y. Teng, Is It Time to Start Transitioning From 2D to 3D Cell Culture?, *Front. Mol. Biosci.*, 2020, **7**, 33.
  - 19 N. A. Peppas, *Biomedical applications of hydrogels handbook*, Springer Science & Business Media, 2010.
  - 20 Y. Osada, J. Ping Gong and Y. Tanaka, Polymer Gels, *J. Macromol. Sci., Part C*, 2004, **44**(1), 87–112.
  - 21 H. Chavda and C. Patel, Effect of crosslinker concentration on characteristics of superporous hydrogel, *Int. J. Pharm. Invest.*, 2011, **1**(1), 17–21.
  - 22 C. Dong and Y. Lv, Application of Collagen Scaffold in Tissue Engineering: Recent Advances and New Perspectives, *Polymers*, 2016, **8**(2), 42.
  - 23 H. Liu, Y. Wang, K. Cui, Y. Guo, X. Zhang and J. Qin, Advances in Hydrogels in Organoids and Organs-on-a-Chip, *Adv. Mater.*, 2019, **31**(50), 1902042.
  - 24 S. T. Kreger, B. J. Bell, J. Bailey, E. Stites, J. Kuske, B. Waisner and S. L. Voytik-Harbin, Polymerization and matrix physical properties as important design considerations for soluble collagen formulations, *Biopolymers*, 2010, **93**(8), 690–707.
  - 25 K. Y. Lee and D. J. Mooney, *Hydrogels for tissue engineering*, 2001, (0009-2665 (print)).
  - 26 X. Jia and K. L. Kiick, Hybrid multicomponent hydrogels for tissue engineering, *Macromol. Biosci.*, 2009, **9**(2), 140–156.
  - 27 C. H. Chuang, R. Z. Lin, J. M. Melero-Martin and Y. C. Chen, Comparison of covalently and physically cross-linked collagen hydrogels on mediating vascular network formation for engineering adipose tissue, *Artif. Cells, Nanomed., Biotechnol.*, 2018, **46**(Suppl 3), S434–S447.
  - 28 S. R. Caliari and J. A. Burdick, A practical guide to hydrogels for cell culture, *Nat. Methods*, 2016, **13**(5), 405–414.
  - 29 S. Utech and A. R. Boccaccini, A review of hydrogel-based composites for biomedical applications: enhancement of hydrogel properties by addition of rigid inorganic fillers, *J. Mater. Sci.*, 2016, **51**(1), 271–310.
  - 30 H. Lu, T. Hoshiba, N. Kawazoe, I. Koda, M. Song and G. Chen, Cultured cell-derived extracellular matrix scaffolds for tissue engineering, *Biomaterials*, 2011, **32**(36), 9658–9666.
  - 31 M. Cavo, M. Caria, I. Pulsoni, F. Beltrame, M. Fato and S. Scaglione, A new cell-laden 3D Alginate-Matrigel hydrogel resembles human breast cancer cell malignant morphology, spread and invasion capability observed “in vivo”, *Sci. Rep.*, 2018, **8**(1), 5333.
  - 32 D. Dippold, A. Cai, M. Hardt, A. R. Boccaccini, R. E. Horch, J. P. Beier and D. W. Schubert, Investigation of the batch-to-batch inconsistencies of Collagen in PCL-Collagen nanofibers, *Mater. Sci. Eng., C*, 2019, **95**, 217–225.
  - 33 C. Tang, B. D. Holt, Z. M. Wright, A. M. Arnold, A. C. Moy and S. A. Sydlík, Injectable amine functionalized graphene and chondroitin sulfate hydrogel with potential for cartilage regeneration, *J. Mater. Chem. B*, 2019, **7**(15), 2442–2453.
  - 34 S. Ricard-Blum, The collagen family, *Cold Spring Harbor Perspect. Biol.*, 2011, **3**(1), a004978, DOI: 10.1101/cshperspect.a004978.
  - 35 P. Fratzl, *Collagen*, Springer US, 2008.
  - 36 J. M. Maki, Lysyl oxidases in mammalian development and certain pathological conditions, *Histol. Histopathol.*, 2009, **24**(5), 651–660.
  - 37 M. Meyer, Processing of collagen based biomaterials and the resulting materials properties, *Biomed. Eng. Online*, 2019, **18**(1), 24.
  - 38 M. Schmidt, R. Dornelles, R. Mello, E. Kubota, M. Mazutti, A. Kempka and I. Demiate, Collagen extraction process, *Int. Food Res. J.*, 2016, **23**(3), 913–922.
  - 39 S. Cersoy, A. Zazzo, M. Lebon, J. Rofes and S. Zirah, Collagen Extraction and Stable Isotope Analysis of Small Vertebrate Bones: A Comparative Approach, *Radiocarbon*, 2017, **59**, 679–694.
  - 40 D. Liu, G. Wei, T. Li, J. Hu, N. Lu, J. M. Regenstein and P. Zhou, Effects of alkaline pretreatments and acid extraction conditions on the acid-soluble collagen from grass carp (*Ctenopharyngodon idella*) skin, *Food Chem.*, 2015, **172**, 836–843.
  - 41 J. Qian, Y. Okada, T. Ogura, K. Tanaka, S. Hattori, S. Ito, J. Satoh, T. Takita and K. Yasukawa, Kinetic Analysis of the Digestion of Bovine Type I Collagen Telopeptides with Porcine Pepsin, *J. Food Sci.*, 2016, **81**(1), C27–C34.
  - 42 D. Hickman, T. J. Sims, C. A. Miles, A. J. Bailey, M. de Mari and M. Koopmans, Isinglass/collagen: denaturation and functionality, *J. Biotechnol.*, 2000, **79**(3), 245–257.
  - 43 W. Song, Extraction Optimization and Characterization of Collagen from the Lung of Soft-Shelled Turtle *Pelodiscus Sinensis*, *Int. J. Nutr. Food Sci.*, 2014, **3**, 270.
  - 44 H. Yang and Z. Shu, The extraction of collagen protein from pigskin, *J. Chem. Pharm. Res.*, 2014, **6**(2), 683–687.
  - 45 P. Noitup, W. Garnjanagoonchorn and M. T. Morrissey, Fish Skin Type I Collagen, *J. Aquat. Food Prod. Technol.*, 2005, **14**(1), 17–28.
  - 46 C. Paola, A. Camila, C. Ana, O. Marlon, S. Diego, R. Zuluaga, G. Beatriz and C. Cristina, Functional textile finishing of type I collagen isolated from bovine bone for potential healthtech, *Heliyon*, 2019, **5**, e01260.

- 47 T. Nagai, Y. Tanoue, N. Kai and N. Suzuki, Characterization of collagen from emu (*Dromaius novaehollandiae*) skins, *J. Food Sci. Technol.*, 2015, **52**(4), 2344–2351.
- 48 W. Liu, Y. Zhang, N. Cui and T. Wang, Extraction and characterization of pepsin-solubilized collagen from snakehead (*Channa argus*) skin: Effects of hydrogen peroxide pretreatments and pepsin hydrolysis strategies, *Process Biochem.*, 2019, **76**, 194–202.
- 49 J. H. Sung, J. Yu, D. Luo, M. L. Shuler and J. C. March, Microscale 3-D hydrogel scaffold for biomimetic gastrointestinal (GI) tract model, *Lab Chip*, 2011, **11**(3), 389–392.
- 50 A. Khademhosseini and R. Langer, Microengineered hydrogels for tissue engineering, *Biomaterials*, 2007, **28**(34), 5087–5092.
- 51 M. Virumbrales-Muñoz, J. M. Ayuso, M. Olave, R. Monge, D. de Miguel, L. Martínez-Lostao, S. Le Gac, M. Doblare, I. Ochoa and L. J. Fernandez, Multiwell capillarity-based microfluidic device for the study of 3D tumour tissue-2D endothelium interactions and drug screening in co-culture models, *Sci. Rep.*, 2017, **7**(1), 11998.
- 52 G. Adriani, D. Ma, A. Pavesi, R. D. Kamm and E. L. K. Goh, A 3D neurovascular microfluidic model consisting of neurons, astrocytes and cerebral endothelial cells as a blood-brain barrier, *Lab Chip*, 2017, **17**(3), 448–459.
- 53 A. Pavesi, A. T. Tan, S. Koh, A. Chia, M. Colombo, E. Antonicchia, C. Miccolis, E. Ceccarello, G. Adriani, M. T. Raimondi, R. D. Kamm and A. Bertolotti, A 3D microfluidic model for preclinical evaluation of TCR-engineered T cells against solid tumors, *JCI Insight*, 2017, **2**(12), e89762, DOI: 10.1172/jci.insight.89762.
- 54 S.-Y. Jeong, J.-H. Lee, Y. Shin, S. Chung and H.-J. Kuh, Co-Culture of Tumor Spheroids and Fibroblasts in a Collagen Matrix-Incorporated Microfluidic Chip Mimics Reciprocal Activation in Solid Tumor Microenvironment, *PLoS One*, 2016, **11**(7), e0159013.
- 55 Y. Zhao, H. Zeng, J. Nam and S. Agarwal, Fabrication of skeletal muscle constructs by topographic activation of cell alignment, *Biotechnol. Bioeng.*, 2009, **102**(2), 624–631.
- 56 W. Zhu, X. Qu, J. Zhu, X. Ma, S. Patel, J. Liu, P. Wang, C. S. E. Lai, M. Gou, Y. Xu, K. Zhang and S. Chen, Direct 3D bioprinting of prevascularized tissue constructs with complex microarchitecture, *Biomaterials*, 2017, **124**, 106–115.
- 57 G. Agrawal, A. Aung and S. Varghese, Skeletal muscle-on-a-chip: an in vitro model to evaluate tissue formation and injury, *Lab Chip*, 2017, **17**(20), 3447–3461.
- 58 A. Skardal, M. Devarasetty, S. Soker and A. R. Hall, In situ patterned micro 3D liver constructs for parallel toxicology testing in a fluidic device, *Biofabrication*, 2015, **7**(3), 031001.
- 59 M. Cabodi, N. W. Choi, J. P. Gleghorn, C. S. Lee, L. J. Bonassar and A. D. Stroock, A microfluidic biomaterial, *J. Am. Chem. Soc.*, 2005, **127**(40), 13788–13789.
- 60 J. V. Green, T. Kniazeva, M. Abedi, D. S. Sokhey, M. E. Taslim and S. K. Murthy, Effect of channel geometry on cell adhesion in microfluidic devices, *Lab Chip*, 2009, **9**(5), 677–685.
- 61 J. He, R. Chen, Y. Lu, L. Zhan, Y. Liu, D. Li and Z. Jin, Fabrication of circular microfluidic network in enzymatically-crosslinked gelatin hydrogel, *Mater. Sci. Eng., C*, 2016, **59**, 53–60.
- 62 K. Mogi and T. Fujii, A novel assembly technique with semi-automatic alignment for PDMS substrates, *Lab Chip*, 2013, **13**(6), 1044–1047.
- 63 S. W. Lee and S. S. Lee, Shrinkage ratio of PDMS and its alignment method for the wafer level process, *Microsyst. Technol.*, 2008, **14**(2), 205–208.
- 64 A. D. Wong and P. C. Searson, Live-Cell Imaging of Invasion and Intravasation in an Artificial Microvessel Platform, *Cancer Res.*, 2014, **74**(17), 4937.
- 65 R. M. Linville, J. G. DeStefano, M. B. Sklar, Z. Xu, A. M. Farrell, M. I. Bogorad, C. Chu, P. Walczak, L. Cheng, V. Mahairaki, K. A. Whartenby, P. A. Calabresi and P. C. Searson, Human iPSC-derived blood-brain barrier microvessels: validation of barrier function and endothelial cell behavior, *Biomaterials*, 2019, **190–191**, 24–37.
- 66 V. K. Lee, D. Y. Kim, H. Ngo, Y. Lee, L. Seo, S. S. Yoo, P. A. Vincent and G. Dai, Creating perfused functional vascular channels using 3D bio-printing technology, *Biomaterials*, 2014, **35**(28), 8092–8102.
- 67 A. Tocchio, M. Tamplenizza, F. Martello, I. Gerges, E. Rossi, S. Argenti, S. Rodighiero, W. Zhao, P. Milani and C. Lenardi, Versatile fabrication of vascularizable scaffolds for large tissue engineering in bioreactor, *Biomaterials*, 2015, **45**, 124–131.
- 68 N. Contessi Negrini, M. Bonnetier, G. Giatsidis, D. P. Orgill, S. Farè and B. Marelli, Tissue-mimicking gelatin scaffolds by alginate sacrificial templates for adipose tissue engineering, *Acta Biomater.*, 2019, **87**, 61–75.
- 69 A. K. Miri, I. Mirzaee, S. Hassan, S. Mesbah Oskui, D. Nieto, A. Khademhosseini and Y. S. Zhang, Effective bioprinting resolution in tissue model fabrication, *Lab Chip*, 2019, **19**(11), 2019–2037.
- 70 X. Cao, R. Ashfaq, F. Cheng, S. Maharjan, J. Li, G. Ying, S. Hassan, H. Xiao, K. Yue, Y. S. Zhang and A. Tumor-on-a-Chip System, with Bioprinted Blood and Lymphatic Vessel Pair, *Adv. Funct. Mater.*, 2019, **29**(31), 1807173.
- 71 B. Grigoryan, S. J. Paulsen, D. C. Corbett, D. W. Sazer, C. L. Fortin, A. J. Zaita, P. T. Greenfield, N. J. Calafat, J. P. Gounley, A. H. Ta, F. Johansson, A. Randles, J. E. Rosenkrantz, J. D. Louis-Rosenberg, P. A. Galie, K. R. Stevens and J. S. Miller, Multivascular networks and functional intravascular topologies within biocompatible hydrogels, *Science*, 2019, **364**(6439), 458.
- 72 L. Ruiz-Cantu, A. Gleadall, C. Faris, J. Segal, K. Shakesheff and J. Yang, Multi-material 3D bioprinting of porous constructs for cartilage regeneration, *Mater. Sci. Eng., C*, 2020, **109**, 110578.
- 73 H.-W. Kang, S. J. Lee, I. K. Ko, C. Kengla, J. J. Yoo and A. Atala, A 3D bioprinting system to produce human-scale tissue constructs with structural integrity, *Nat. Biotechnol.*, 2016, **34**(3), 312–319.
- 74 N. Arumugasaamy, H. Baker, D. Kaplan, P. Kim and J. Fisher, *Fabrication and Printing of Multi-material Hydrogels*, 2016, pp. 1–34.
- 75 D. C. Corbett, E. Olszewski and K. Stevens, A FRESH Take on Resolution in 3D Bioprinting, *Trends Biotechnol.*, 2019, **37**(11), 1153–1155.

- 76 S. Massa, M. A. Sakr, J. Seo, P. Bandaru, A. Arneri, S. Bersini, E. Zare-Eelanjegh, E. Jalilian, B. H. Cha, S. Antona, A. Enrico, Y. Gao, S. Hassan, J. P. Acevedo, M. R. Dokmeci, Y. S. Zhang, A. Khademhosseini and S. R. Shin, Bioprinted 3D vascularized tissue model for drug toxicity analysis, *Biomicrofluidics*, 2017, **11**(4), 044109.
- 77 F. Yanagawa, S. Sugiura and T. Kanamori, Hydrogel micro-fabrication technology toward three dimensional tissue engineering, *Regener. Ther.*, 2016, **3**, 45–57.
- 78 L. E. Bertassoni, J. C. Cardoso, V. Manoharan, A. L. Cristino, N. S. Bhise, W. A. Araujo, P. Zorlutuna, N. E. Vrana, A. M. Ghaemmaghami, M. R. Dokmeci and A. Khademhosseini, Direct-write bioprinting of cell-laden methacrylated gelatin hydrogels, *Biofabrication*, 2014, **6**(2), 024105.
- 79 A. Blaeser, D. F. D. Campos, U. Puster, W. Richtering, M. M. Stevens and H. Fischer, Controlling Shear Stress in 3D Bioprinting is a Key Factor to Balance Printing Resolution and Stem Cell Integrity, *Adv. Healthcare Mater.*, 2016, **5**(3), 326–333.
- 80 J. Gopinathan and I. Noh, Recent trends in bioinks for 3D printing, *Biomater. Res.*, 2018, **22**(1), 11.
- 81 M. Hospodiuk, M. Dey, D. Sosnoski and I. Ozbolat, The bioink: A comprehensive review on bioprintable materials, *Biotechnol. Adv.*, 2017, **35**, 217–239.
- 82 C. M. Livoti and J. R. Morgan, Self-assembly and tissue fusion of toroid-shaped minimal building units, *Tissue Eng., Part A*, 2010, **16**(6), 2051–2061.
- 83 N. E. Fedorovich, J. R. De Wijn, A. J. Verbout, J. Alblas and W. J. Dhert, Three-dimensional fiber deposition of cell-laden, viable, patterned constructs for bone tissue printing, *Tissue Eng., Part A*, 2008, **14**(1), 127–133.
- 84 F. Kreimendahl, M. Köpf, A. L. Thiebes, D. F. Duarte Campos, A. Blaeser, T. Schmitz-Rode, C. Apel, S. Jockenhoevel and H. Fischer, Three-Dimensional Printing and Angiogenesis: Tailored Agarose-Type I Collagen Blends Comprise Three-Dimensional Printability and Angiogenesis Potential for Tissue-Engineered Substitutes, *Tissue Eng., Part C*, 2017, **23**(10), 604–615.
- 85 E. Axpe and M. L. Oyen, Applications of Alginate-Based Bioinks in 3D Bioprinting, *Int. J. Mol. Sci.*, 2016, **17**(12), 1976.
- 86 W. Jia, P. S. Gungor-Ozkerim, Y. S. Zhang, K. Yue, K. Zhu, W. Liu, Q. Pi, B. Byambaa, M. R. Dokmeci, S. R. Shin and A. Khademhosseini, Direct 3D bioprinting of perfusable vascular constructs using a blend bioink, *Biomaterials*, 2016, **106**, 58–68.
- 87 K. Y. Lee and D. J. Mooney, Alginate: properties and biomedical applications, *Prog. Polym. Sci.*, 2012, **37**(1), 106–126.
- 88 X. Yu, J. Xiao and F. Dang, Surface Modification of Poly(dimethylsiloxane) Using Ionic Complementary Peptides to Minimize Nonspecific Protein Adsorption, *Langmuir*, 2015, **31**(21), 5891–5898.
- 89 W.-G. Koh, A. Revzin, A. Simonian, T. Reeves and M. Pishko, Control of Mammalian Cell and Bacteria Adhesion on Substrates Micropatterned with Poly(ethylene glycol) Hydrogels, *Biomed. Microdevices*, 2003, **5**(1), 11–19.
- 90 H. J. Lee, H.-S. Kim, H. O. Kim and W.-G. Koh, Micro-patterns of double-layered nanofiber scaffolds with dual functions of cell patterning and metabolite detection, *Lab Chip*, 2011, **11**(17), 2849–2857.
- 91 J. Xue, T. Wu, Y. Dai and Y. Xia, Electrospinning and Electrospun Nanofibers: Methods, Materials, and Applications, *Chem. Rev.*, 2019, **119**(8), 5298–5415.
- 92 K. Zhao, W. Wang, Y. Y. Yang, K. Wang and D. G. Yu, From Taylor cone to solid nanofiber in tri-axial electrospinning: Size relationships, *Results Phys.*, 2019, **15**, 102770.
- 93 A. Khalf and S. V. Madihally, Recent advances in multiaxial electrospinning for drug delivery, *Eur. J. Pharm. Biopharm.*, 2017, **112**, 1–17.
- 94 M. Zündel, A. E. Ehret and E. Mazza, The multiscale stiffness of electrospun substrates and aspects of their mechanical biocompatibility, *Acta Biomater.*, 2019, **84**, 146–158.
- 95 F. Topuz and T. Uyar, Electrospinning of gelatin with tunable fiber morphology from round to flat/ribbon, *Mater. Sci. Eng., C*, 2017, **80**, 371–378.
- 96 N. Bhardwaj and S. C. Kundu, Electrospinning: A fascinating fiber fabrication technique, *Biotechnol. Adv.*, 2010, **28**(3), 325–347.
- 97 D. Garlotta, A Literature Review of Poly(Lactic Acid), *J. Polym. Environ.*, 2001, **9**(2), 63–84.
- 98 M. Labet and W. Thielemans, Synthesis of polycaprolactone: a review, *Chem. Soc. Rev.*, 2009, **38**(12), 3484–3504.
- 99 J. Venugopal and S. Ramakrishna, Applications of polymer nanofibers in biomedicine and biotechnology, *Appl. Biochem. Biotechnol.*, 2005, **125**(3), 147–157.
- 100 H. Yoshimoto, Y. M. Shin, H. Terai and J. P. Vacanti, A biodegradable nanofiber scaffold by electrospinning and its potential for bone tissue engineering, *Biomaterials*, 2003, **24**(12), 2077–2082.
- 101 S. Yan, B. Napiwocki, Y. Xu, J. Zhang, X. Zhang, X. Wang, W. C. Crone, Q. Li and L.-S. Turng, Wavy small-diameter vascular graft made of eggshell membrane and thermoplastic polyurethane, *Mater. Sci. Eng., C*, 2020, **107**, 110311.
- 102 J. Chen, T. Zhang, W. Hua, P. Li and X. Wang, 3D Porous poly(lactic acid)/regenerated cellulose composite scaffolds based on electrospun nanofibers for biomineralization, *Colloids Surf., A*, 2020, **585**, 124048.
- 103 J. Baek, E. Lee, M. K. Lotz and D. D. D'Lima, Bioactive proteins delivery through core-shell nanofibers for meniscal tissue regeneration, *Nanomedicine*, 2020, **23**, 102090.
- 104 S. Kim and C. Cha, Enhanced mechanical and electrical properties of heteroscaled hydrogels infused with aqueous-dispersible hybrid nanofibers, *Biofabrication*, 2019, **12**(1), 015020.
- 105 L. Wu, Y. Gu, L. Liu, J. Tang, J. Mao, K. Xi, Z. Jiang, Y. Zhou, Y. Xu, L. Deng, L. Chen and W. Cui, Hierarchical micro/nanofibrous membranes of sustained releasing VEGF for periosteal regeneration, *Biomaterials*, 2020, **227**, 119555.
- 106 K. H. Song, S.-J. Heo, A. P. Peredo, M. D. Davidson, R. L. Mauck and J. A. Burdick, Influence of Fiber Stiffness on Meniscal Cell Migration into Dense Fibrous Networks, *Adv. Healthcare Mater.*, 2019, 1901228.

- 107 K. Roshanbinfar, L. Vogt, F. Ruther, J. A. Roether, A. R. Boccaccini and F. B. Engel, Nanofibrous Composite with Tailorable Electrical and Mechanical Properties for Cardiac Tissue Engineering, *Adv. Funct. Mater.*, 2020, **30**(7), 1908612.
- 108 N. C. Islas-Arteaga, A. Raya Rivera, D. R. Esquiliano Rendon, J. Morales-Corona, P. G. Ontiveros-Nevarés, M. G. Flores Sánchez, C. Mojica-Cardoso and R. Olayo, Electrospun scaffolds with surfaces modified by plasma for regeneration of articular cartilage tissue: a pilot study in rabbit, *Int. J. Polym. Mater. Polym. Biomater.*, 2019, **68**(18), 1089–1098.
- 109 C. B. Horner, M. Maldonado, Y. Tai, R. M. I. K. Rony and J. Nam, Spatially Regulated Multiphenotypic Differentiation of Stem Cells in 3D via Engineered Mechanical Gradient, *ACS Appl. Mater. Interfaces*, 2019, **11**(49), 45479–45488.
- 110 S. Nagam Hanumantharao, N. Alinezhadbalalami, S. Kannan, M. Friske and S. Rao, Electrospun acellular scaffolds for mimicking the natural anisotropy of the extracellular matrix, *RSC Adv.*, 2019, **9**(69), 40190–40195.
- 111 B. R. Shambaugh, D. V. Papavassiliou and R. L. Shambaugh, Next-Generation Modeling of Melt Blowing, *Ind. Eng. Chem. Res.*, 2011, **50**(21), 12233–12245.
- 112 P. Ginestra, Manufacturing of polycaprolactone - Graphene fibers for nerve tissue engineering, *J. Mech. Behav. Biomed. Mater.*, 2019, **100**, 103387.
- 113 J. A. Reid and A. Callanan, Influence of aorta extracellular matrix in electrospun polycaprolactone scaffolds, *J. Appl. Polym. Sci.*, 2019, **136**(44), 48181.
- 114 S. Fujita, Y. Wakuda, M. Matsumura and S.-i. Suze, Geometrically customizable alginate hydrogel nanofibers for cell culture platforms, *J. Mater. Chem. B*, 2019, **7**(42), 6556–6563.
- 115 H. Nazari, A. Heirani-Tabasi, M. Hajiabbas, M. Salimi Bani, M. Nazari, V. Pirhajati Mahabadi, I. Rad, M. Kehtari, S. H. Ahmadi Tafti and M. Soleimani, Incorporation of SPION-casein core-shells into silk-fibroin nanofibers for cardiac tissue engineering, *J. Cell. Biochem.*, 2019, **121**(4), 2981–2993.
- 116 R. Li, A. McCarthy, Y. S. Zhang and J. Xie, Decorating 3D Printed Scaffolds with Electrospun Nanofiber Segments for Tissue Engineering, *Adv. Biosyst.*, 2019, **3**(12), 1900137.
- 117 S. Jana, A. Bhagia and A. Lerman, Optimization of polycaprolactone fibrous scaffold for heart valve tissue engineering, *Biomed. Mater.*, 2019, **14**(6), 065014.
- 118 M. Azizi, M. Navidbakhsh, S. Hosseinzadeh and M. Sajjadi, Cardiac cell differentiation of muscle satellite cells on aligned composite electrospun polyurethane with reduced graphene oxide, *J. Polym. Res.*, 2019, **26**(11), 258.
- 119 A. Abedi, M. Hasanzadeh and L. Tayebi, Conductive nanofibrous Chitosan/PEDOT:PSS tissue engineering scaffolds, *Mater. Chem. Phys.*, 2019, **237**, 121882.
- 120 M. Li, X. Zhang, W. Jia, Q. Wang, Y. Liu, X. Wang, C. Wang, J. Jiang, G. Gu, Z. Guo and Z. Chen, Improving in vitro biocompatibility on biomimetic mineralized collagen bone materials modified with hyaluronic acid oligosaccharide, *Mater. Sci. Eng., C*, 2019, **104**, 110008.
- 121 H. Lee, W. Kim, J. Lee, J. J. Yoo, G. H. Kim and S. J. Lee, Effect of Hierarchical Scaffold Consisting of Aligned dECM Nanofibers and Poly(lactide-co-glycolide) Struts on the Orientation and Maturation of Human Muscle Progenitor Cells, *ACS Appl. Mater. Interfaces*, 2019, **11**(43), 39449–39458.
- 122 L. Mohammadzadeh, R. Rahbarghazi, R. Salehi and M. Mahkam, A novel egg-shell membrane based hybrid nanofibrous scaffold for cutaneous tissue engineering, *J. Biol. Eng.*, 2019, **13**, 79.
- 123 H. Nazari, A. Heirani-Tabasi, M. S. Alavijeh, Z. S. Jeshvaghani, E. Esmaeili, S. Hosseinzadeh, F. Mohabatpour, B. Taheri, S. H. A. Tafti and M. Soleimani, Nanofibrous Composites Reinforced by MoS<sub>2</sub> Nanosheets as a Conductive Scaffold for Cardiac Tissue Engineering, *ChemistrySelect*, 2019, **4**(39), 11557–11563.
- 124 D. Kim, S. Eom, S. M. Park, H. Hong and D. S. Kim, A collagen gel-coated, aligned nanofiber membrane for enhanced endothelial barrier function, *Sci. Rep.*, 2019, **9**(1), 14915.
- 125 W. Chen, Y. Xu, Y. Liu, Z. Wang, Y. Li, G. Jiang, X. Mo and G. Zhou, Three-dimensional printed electrospun fiber-based scaffold for cartilage regeneration, *Mater. Des.*, 2019, **179**, 107886.
- 126 Y. Hou, X. Wang, Z. Zhang, J. Luo, Z. Cai, Y. Wang and Y. Li, Repairing Transected Peripheral Nerve Using a Biomimetic Nerve Guidance Conduit Containing Intraluminal Sponge Fillers, *Adv. Healthcare Mater.*, 2019, **8**(21), 1900913.
- 127 Q. P. Pham, U. Sharma and A. G. Mikos, Electrospun Poly( $\epsilon$ -caprolactone) Microfiber and Multilayer Nanofiber/Microfiber Scaffolds: Characterization of Scaffolds and Measurement of Cellular Infiltration, *Biomacromolecules*, 2006, **7**(10), 2796–2805.
- 128 K.-C. Tang, K.-C. Yang, C.-W. Lin, Y.-K. Chen, T.-Y. Lu, H.-Y. Chen, N.-C. Cheng and J. Yu, Human Adipose-Derived Stem Cell Secreted Extracellular Matrix Incorporated into Electrospun Poly(Lactic-co-Glycolic Acid) Nanofibrous Dressing for Enhancing Wound Healing, *Polymers*, 2019, **11**(10), 1609.
- 129 A. Malakpour Permlid, P. Roci, E. Fredlund, F. Fält, E. Önell, F. Johansson and S. Oredsson, Unique animal friendly 3D culturing of human cancer and normal cells, *Toxicol. In Vitro*, 2019, **60**, 51–60.
- 130 T. Li, L. Tian, S. Liao, X. Ding, S. A. Irvine and S. Ramakrishna, Fabrication, mechanical property and in vitro evaluation of poly (L-lactic acid-co- $\epsilon$ -caprolactone) core-shell nanofiber scaffold for tissue engineering, *J. Mech. Behav. Biomed. Mater.*, 2019, **98**, 48–57.
- 131 R. Sobreiro-Almeida, D. R. Fonseca and N. M. Neves, Extracellular matrix electrospun membranes for mimicking natural renal filtration barriers, *Mater. Sci. Eng., C*, 2019, **103**, 109866.
- 132 A. Yin, X. Lan, W. Zhuang, Z. Tang, Y. Li and Y. Wang, PEGylated chitosan and PEGylated PLCL for blood vessel repair: An in vitro study, *J. Biomater. Appl.*, 2019, **34**(6), 778–789.
- 133 J. P. Chan, K. G. Battiston and J. P. Santerre, Synthesis and characterization of electrospun nanofibrous tissue engineering scaffolds generated from in situ polymerization of ionomeric polyurethane composites, *Acta Biomater.*, 2019, **96**, 161–174.



- 134 M. Idini, P. Wieringa, S. Rocchiccioli, G. Nieddu, N. Ucciferri, M. Formato, A. Lepedda and L. Moroni, Glycosaminoglycan functionalization of electrospun scaffolds enhances Schwann cell activity, *Acta Biomater.*, 2019, **96**, 188–202.
- 135 X. Jing, H. Li, H.-Y. Mi, Y.-J. Liu and Y.-M. Tan, Fabrication of fluffy shish-kebab structured nanofibers by electrospinning, CO<sub>2</sub> escaping foaming and controlled crystallization for biomimetic tissue engineering scaffolds, *Chem. Eng. J.*, 2019, **372**, 785–795.
- 136 G. Sandri, S. Rossi, M. C. Bonferoni, D. Miele, A. Faccendini, E. Del Favero, E. Di Cola, A. Icaro Cornaglia, C. Boselli, T. Luxbacher, L. Malavasi, L. Cantu' and F. Ferrari, Chitosan/glycosaminoglycan scaffolds for skin reparation, *Carbohydr. Polym.*, 2019, **220**, 219–227.
- 137 N. Watcharajittanont, C. Putson, P. Pripatnanont and J. Meesane, Electrospun polyurethane fibrous membranes of mimicked extracellular matrix for periodontal ligament: Molecular behavior, mechanical properties, morphology, and osseointegration, *J. Biomater. Appl.*, 2019, **34**(6), 753–762.
- 138 R. Rynkevic, P. Martins, A. Fernandes, J. Vange, M. R. Gallego, R. A. Wach, T. Mes, A. W. Bosman and J. Deprest, In vitro simulation of in vivo degradation and cyclic loading of novel degradable electrospun meshes for prolapse repair, *Polym. Test.*, 2019, **78**, 105957.
- 139 H. S. Cho, I. J. Kim, S. C. Kim, H. C. Park and G. I. Kim, Harnessing the Topography of 3D Spongy-Like Electrospun Bundled Fibrous Scaffold via a Sharply Inclined Array Collector, *Polymers*, 2019, **11**(9), 1444.
- 140 Y. Wang, Z. Guo, Y. Qian, Z. Zhang, L. Lyu, Y. Wang and F. Ye, Study on the Electrospinning of Gelatin/Pullulan Composite Nanofibers, *Polymers*, 2019, **11**(9), 1424.
- 141 C. G. Elliott, J. Wang, J. T. Walker, S. Michelsons, J. Dunmore-Buyze, M. Drangova, A. Leask and D. W. Hamilton, Periostin and CCN2 Scaffolds Promote the Wound Healing Response in the Skin of Diabetic Mice, *Tissue Eng., Part A*, 2018, **25**(17–18), 1326–1339.
- 142 J. Hodge and C. Quint, The improvement of cell infiltration in an electrospun scaffold with multiple synthetic biodegradable polymers using sacrificial PEO microparticles, *J. Biomed. Mater. Res., Part A*, 2019, **107**(9), 1954–1964.
- 143 J. Jiménez Vázquez and E. San Martín Martínez, Collagen and elastin scaffold by electrospinning for skin tissue engineering applications, *J. Mater. Res.*, 2019, **34**(16), 2819–2827.
- 144 F. Yongcong, T. Zhang, L. Liverani, A. R. Boccaccini and W. Sun, Novel biomimetic fiber incorporated scaffolds for tissue engineering, *J. Biomed. Mater. Res., Part A*, 2019, **107**(12), 2694–2705.
- 145 H. Ye, J. Zhu, D. Deng, S. Jin, J. Li and Y. Man, Enhanced osteogenesis and angiogenesis by PCL/chitosan/Sr-doped calcium phosphate electrospun nanocomposite membrane for guided bone regeneration, *J. Biomater. Sci., Polym. Ed.*, 2019, **30**(16), 1505–1522.
- 146 Y. Li, Z. Xiao, Y. Zhou, S. Zheng, Y. An, W. Huang, H. He, Y. Yang, S. Li, Y. Chen, J. Xiao and J. Wu, Controlling the Multiscale Network Structure of Fibers To Stimulate Wound Matrix Rebuilding by Fibroblast Differentiation, *ACS Appl. Mater. Interfaces*, 2019, **11**(31), 28377–28386.
- 147 A. Sensini, L. Cristofolini, A. Zucchelli, M. L. Focarete, C. Gualandi, A. De Mori, A. P. Kao, M. Roldo, G. Blunn and G. Tozzi, Hierarchical electrospun tendon-ligament bioinspired scaffolds induce changes in fibroblasts morphology under static and dynamic conditions, *J. Microsc.*, 2019, **277**(3), 160–169.
- 148 M. D. Davidson, K. H. Song, M.-H. Lee, J. Llewellyn, Y. Du, B. M. Baker, R. G. Wells and J. A. Burdick, Engineered Fibrous Networks To Investigate the Influence of Fiber Mechanics on Myofibroblast Differentiation, *ACS Biomater. Sci. Eng.*, 2019, **5**(8), 3899–3908.
- 149 J. A. Reid and A. Callanan, Hybrid cardiovascular sourced extracellular matrix scaffolds as possible platforms for vascular tissue engineering, *J. Biomed. Mater. Res., Part B*, 2019, **108**(3), 910–924.
- 150 C. A. Best, J. M. Szafron, K. A. Rocco, J. Zbinden, E. W. Dean, M. W. Maxfield, H. Kurobe, S. Tara, P. S. Bagi, B. V. Udelsman, R. Khosravi, T. Yi, T. Shinoka, J. D. Humphrey and C. K. Breuer, Differential outcomes of venous and arterial tissue engineered vascular grafts highlight the importance of coupling long-term implantation studies with computational modeling, *Acta Biomater.*, 2019, **94**, 183–194.
- 151 N. Azim, A. Kundu, M. Royse, Y. Y. L. Sip, M. Young, S. Santra, L. Zhai and S. Rajaraman, Fabrication and Characterization of a 3D Printed, MicroElectrodes Platform With Functionalized Electrospun Nano-Scaffolds and Spin Coated 3D Insulation Towards Multi-Functional Biosystems, *J. Microelectromech. Syst.*, 2019, **28**(4), 606–618.
- 152 M. Vardiani, M. Gholipourmalekabadi, M. Ghaffari Novin, M. Koruji, H. Ghasemi Hamidabadi, M. Salimi and H. Nazarian, Three-dimensional electrospun gelatin scaffold coseeded with embryonic stem cells and sertoli cells: A promising substrate for in vitro coculture system, *J. Cell. Biochem.*, 2019, **120**(8), 12508–12518.
- 153 W. Jia, M. Li, L. Kang, G. Gu, Z. Guo and Z. Chen, Fabrication and Comprehensive Characterization of Biomimetic Extracellular Matrix Electrospun Scaffold for Vascular Tissue Engineering Applications, *J. Mater. Sci.*, 2019, **54**(15), 10871–10883.
- 154 A. Ghasemi, R. Imani, M. Yousefzadeh, S. Bonakdar, A. Solouk and H. Fakhzadeh, Studying the Potential Application of Electrospun Polyethylene Terephthalate/Graphene Oxide Nanofibers as Electroconductive Cardiac Patch, *Macromol. Mater. Eng.*, 2019, **304**(8), 1900187.
- 155 R. E. Young, J. Graf, I. Miserocchi, R. M. Van Horn, M. B. Gordon, C. R. Anderson and L. S. Sefcik, Optimizing the alignment of thermoresponsive poly(N-isopropyl acrylamide) electrospun nanofibers for tissue engineering applications: A factorial design of experiments approach, *PLoS One*, 2019, **14**(7), e0219254.
- 156 S. K. Jaganathan, M. P. Mani, P. Prabhakaran, E. Supriyanto and A. F. Ismail, Production, blood compatibility and cytotoxicity evaluation of a single stage non-woven multicomponent

- electrospun scaffold mixed with sesame oil, honey and propolis for skin tissue engineering, *Int. J. Polym. Anal. Charact.*, 2019, **24**(5), 457–474.
- 157 M. I. Hassan and N. Sultana, In vitro cell viability of PHBV/PLGA nanofibrous membrane for tissue engineering, *Malaysian J. Fundament. Appl. Sci.*, 2019, **15**(4), 522–527.
- 158 R. Augustine, A. Hasan, N. K. Patan, A. Augustine, Y. B. Dalvi, R. Varghese, R. N. Unni, N. Kalarikkal, A.-E. Al Moustafa and S. Thomas, Titanium Nanorods Loaded PCL Meshes with Enhanced Blood Vessel Formation and Cell Migration for Wound Dressing Applications, *Macromol. Biosci.*, 2019, **19**(7), 1900058.
- 159 C. Liu, B. Li, X. Mao, Q. Zhang, R. Sun, R. H. Gong and F. Zhou, Controllable Aligned Nanofiber Hybrid Yarns with Enhanced Bioproperties for Tissue Engineering, *Macromol. Mater. Eng.*, 2019, **304**(7), 1900089.
- 160 Z. Li, I. M. Lei, P. Davoodi, L. Huleihel and Y. Y. S. Huang, Solution Formulation and Rheology for Fabricating Extracellular Matrix-Derived Fibers Using Low-Voltage Electrospinning Patterning, *ACS Biomater. Sci. Eng.*, 2019, **5**(7), 3676–3684.
- 161 C. Zhijiang, X. Ping, H. Shiqi and Z. Cong, Soy protein nanoparticles modified bacterial cellulose electrospun nanofiber membrane scaffold by ultrasound-induced self-assembly technique: characterization and cytocompatibility, *Cellulose*, 2019, **26**(10), 6133–6150.
- 162 A. Sadeghi, M. Zandi, M. Pezeshki-Modaress and S. Rajabi, Tough, hybrid chondroitin sulfate nanofibers as a promising scaffold for skin tissue engineering, *Int. J. Biol. Macromol.*, 2019, **132**, 63–75.
- 163 M. M. O. Simbara, A. R. Santos Jr, A. J. P. Andrade and S. M. Malmonge, Comparative study of aligned and non-aligned poly( $\epsilon$ -caprolactone) fibrous scaffolds prepared by solution blow spinning, *J. Biomed. Mater. Res., Part B*, 2019, **107**(5), 1462–1470.
- 164 L. L. Lima, T. B. Taketa, M. M. Beppu, I. M. d. O. Sousa, M. A. Foglio and Á. M. Moraes, Coated electrospun bioactive wound dressings: Mechanical properties and ability to control lesion microenvironment, *Mater. Sci. Eng., C*, 2019, **100**, 493–504.
- 165 H. Du, L. Tao, W. Wang, D. Liu, Q. Zhang, P. Sun, S. Yang and C. He, Enhanced biocompatibility of poly(L-lactide-co-epsilon-caprolactone) electrospun vascular grafts via self-assembly modification, *Mater. Sci. Eng., C*, 2019, **100**, 845–854.
- 166 M. Atrian, M. Kharaziha, R. Emadi and F. Alihosseini, Silk-LAPONITE<sup>®</sup> fibrous membranes for bone tissue engineering, *Appl. Clay Sci.*, 2019, **174**, 90–99.
- 167 X. Luan, H. Wang, Z. Xiang, Z. Ma, J. Zhao, Y. Feng, Q. Shi and J. Yin, Biomimicking Dual-Responsive Extracellular Matrix Restoring Extracellular Balance through the Na/K-ATPase Pathway, *ACS Appl. Mater. Interfaces*, 2019, **11**(23), 21258–21267.
- 168 X. Jing, H. Li, H.-Y. Mi, Y.-J. Liu and Y.-M. Tan, Fabrication of Three-Dimensional Fluffy Nanofibrous Scaffolds for Tissue Engineering via Electrospinning and CO<sub>2</sub> Escaping Foaming, *Ind. Eng. Chem. Res.*, 2019, **58**(22), 9412–9421.
- 169 E. L. Gill, S. Willis, M. Gerigk, P. Cohen, D. Zhang, X. Li and Y. Y. S. Huang, Fabrication of Designable and Suspended Microfibers via Low-Voltage 3D Micropatterning, *ACS Appl. Mater. Interfaces*, 2019, **11**(22), 19679–19690.
- 170 A. Youssef, A. Hrynevich, L. Fladeland, A. Balles, J. Groll, P. D. Dalton and S. Zabler, The Impact of Melt Electrowritten Scaffold Design on Porosity Determined by X-Ray Microtomography, *Tissue Eng., Part C*, 2019, **25**(6), 367–379.
- 171 B. Aghaei-Ghareh-Bolagh, S. M. Mithieux, M. A. Hiob, Y. Wang, A. Chong and A. S. Weiss, Fabricated tropoelastin-silk yarns and woven textiles for diverse tissue engineering applications, *Acta Biomater.*, 2019, **91**, 112–122.
- 172 A. Fallahi, S. Mandla, T. Kerr-Phillip, J. Seo, R. O. Rodrigues, Y. A. Jodat, R. Samanipour, M. A. Hussain, C. K. Lee, H. Bae, A. Khademhosseini, J. Travas-Sejdic and S. R. Shin, Flexible and Stretchable PEDOT-Embedded Hybrid Substrates for Bioengineering and Sensory Applications, *ChemNanoMat*, 2019, **5**(6), 729–737.
- 173 A. Beishenaliev, S. S. Lim, K. Y. Tshai, P. S. Khiew, H. N. Moh'd Sghayyar and H.-S. Loh, Fabrication and preliminary in vitro evaluation of ultraviolet-crosslinked electrospun fish scale gelatin nanofibrous scaffolds, *J. Mater. Sci.: Mater. Med.*, 2019, **30**(6), 62.
- 174 J. Du, J.-H. Wang, H.-Y. Yu, Y.-Y. Zhang, L.-H. Pu, J.-C. Wang, S.-Y. Lu, S.-H. Chen and T.-H. Zhu, Electrospun Poly(p-dioxanone)/Poly(ester-urethane)ureas Composite Nanofibers for Potential Heart Valve Tissue Reconstruction, *Chin. J. Polym. Sci.*, 2019, **37**(6), 560–569.
- 175 X. Xie, D. Li, C. Su, W. Cong, X. Mo, G. Hou and C. Wang, Functionalized Biomimetic Composite Nanofibrous Scaffolds with Antibacterial and Hemostatic Efficacy for Facilitating Wound Healing, *J. Biomed. Nanotechnol.*, 2019, **15**(6), 1267–1279.
- 176 M. Gluais, J. Clouet, M. Fusellier, C. Decante, C. Moraru, M. Dutilleul, J. Veziere, J. Lesoeur, D. Dumas, J. Abadie, A. Hamel, E. Bord, S. Y. Chew, J. Guicheux and C. Le Visage, In vitro and in vivo evaluation of an electrospun-aligned microfibrillar implant for Annulus fibrosus repair, *Biomaterials*, 2019, **205**, 81–93.
- 177 M. S. Carvalho, J. C. Silva, R. N. Udangawa, J. M. S. Cabral, F. C. Ferreira, C. L. da Silva, R. J. Linhardt and D. Vashishth, Co-culture cell-derived extracellular matrix loaded electrospun microfibrillar scaffolds for bone tissue engineering, *Mater. Sci. Eng., C*, 2019, **99**, 479–490.
- 178 F. T. G. Dias, A. R. Ingracio, N. F. Nicoletti, F. C. Menezes, L. Dall Agnol, D. R. Marinowic, R. M. D. Soares, J. C. da Costa, A. Falavigna and O. Bianchi, Soybean-modified polyamide-6 mats as a long-term cutaneous wound covering, *Mater. Sci. Eng., C*, 2019, **99**, 957–968.
- 179 S. Liu, C. Niu, Z. Xu, Y. Wang, Y. Liang, Y. Zhao, Y. Zhao and Y. Yang, Modulation of myelin formation by combined high affinity with extracellular matrix structure of electrospun silk fibroin nanoscaffolds, *J. Biomater. Sci., Polym. Ed.*, 2019, **30**(12), 1068–1082.
- 180 G. Li, P. Li, Q. Chen, M. P. Mani and S. K. Jaganathan, Enhanced mechanical, thermal and biocompatible nature

- of dual component electrospun nanocomposite for bone tissue engineering, *PeerJ*, 2019, 7, e6986.
- 181 E. Polonio-Alcalá, M. Rabionet, X. Gallardo, D. Angelats, J. Ciurana, S. Ruiz-Martínez and T. Puig, PLA Electrospun Scaffolds for Three-Dimensional Triple-Negative Breast Cancer Cell Culture, *Polymers*, 2019, 11(5), 916.
- 182 J. Fernández, M. Ruiz-Ruiz and J.-R. Sarasua, Electrospun Fibers of Polyester, with Both Nano- and Micron Diameters, Loaded with Antioxidant for Application as Wound Dressing or Tissue Engineered Scaffolds, *ACS Appl. Polym. Mater.*, 2019, 1(5), 1096–1106.
- 183 R. Menezes, S. Hashemi, R. Vincent, G. Collins, J. Meyer, M. Foston and T. L. Arinzeh, Investigation of glycosaminoglycan mimetic scaffolds for neurite growth, *Acta Biomater.*, 2019, 90, 169–178.
- 184 E. Altun, M. O. Aydogdu, S. O. Togay, A. Z. Sengil, N. Ekren, M. E. Haskoylu, E. T. Oner, N. A. Altuncu, G. Ozturk, M. Crabbe-Mann, J. Ahmed, O. Gunduz and M. Edirisinghe, Bioinspired scaffold induced regeneration of neural tissue, *Eur. Polym. J.*, 2019, 114, 98–108.
- 185 M. M. Smoak, A. Han, E. Watson, A. Kishan, K. J. Grande-Allen, E. Cosgriff-Hernandez and A. G. Mikos, Fabrication and Characterization of Electrospun Decellularized Muscle-Derived Scaffolds, *Tissue Eng., Part C*, 2019, 25(5), 276–287.
- 186 T. Yu, S. E. Gleeson, C. Y. Li and M. Marcolongo, Electrospun poly( $\epsilon$ -caprolactone) nanofiber shish kebabs mimic mineralized bony surface features, *J. Biomed. Mater. Res., Part B*, 2019, 107(4), 1141–1149.
- 187 K. H. Patel, A. J. Dunn, M. Talovic, G. J. Haas, M. Marcinczyk, H. Elmashhady, E. G. Kalaf, S. A. Sell and K. Garg, Aligned nanofibers of decellularized muscle ECM support myogenic activity in primary satellite cells in vitro, *Biomed. Mater.*, 2019, 14(3), 035010.
- 188 L. Zhong, D. Hu, Y. Qu, J. Peng, K. Huang, M. Lei, T. Wu, Y. Xiao, Y. Gu and Z. Qian, Preparation of Adenosine-Loaded Electrospun Nanofibers and Their Application in Bone Regeneration, *J. Biomed. Nanotechnol.*, 2019, 15(5), 857–877.
- 189 A. Mirzaei, E. Saburi, M. Islami, A. Ardeshiryajimi, M. D. Omrani, M. Taheri, A. S. Moghadam and S. Ghafouri-Fard, Bladder smooth muscle cell differentiation of the human induced pluripotent stem cells on electrospun Poly(lactide-co-glycolide) nanofibrous structure, *Gene*, 2019, 694, 26–32.
- 190 R. Grant, J. Hallett, S. Forbes, D. Hay and A. Callanan, Blended electrospinning with human liver extracellular matrix for engineering new hepatic microenvironments, *Sci. Rep.*, 2019, 9(1), 6293.
- 191 D. Kumar, S. A. Cain and L. A. Bosworth, Effect of Topography and Physical Stimulus on hMSC Phenotype Using a 3D In Vitro Model, *Nanomaterials*, 2019, 9(4), 522.
- 192 C. Chen, A. D. Townsend, S. A. Sell and R. S. Martin, Microchip-based 3D-cell culture using polymer nanofibers generated by solution blow spinning, *Anal. Methods*, 2017, 9(22), 3274–3283.
- 193 M. Vashaghian, S. J. Zaat, T. H. Smit and J.-P. Roovers, Biomimetic implants for pelvic floor repair, *NeuroUrol. Urodynam.*, 2018, 37(2), 566–580.
- 194 L. Terranova, D. M. Dragusin, R. Mallet, E. Vasile, I.-C. Stancu, C. Behets and D. Chappard, Repair of calvarial bone defects in mice using electrospun polystyrene scaffolds combined with  $\beta$ -TCP or gold nanoparticles, *Micron*, 2017, 93, 29–37.
- 195 M. F. Leong, H. F. Lu, T. C. Lim, C. Du, N. K. L. Ma and A. C. A. Wan, Electrospun polystyrene scaffolds as a synthetic substrate for xeno-free expansion and differentiation of human induced pluripotent stem cells, *Acta Biomater.*, 2016, 46, 266–277.
- 196 I. J. H. Barrientos, G. R. MacKenzie, C. G. Wilson, D. A. Lamprou and P. Coats, Biological Performance of Electrospun Polymer Fibres, *Materials*, 2019, 12(3), 363.
- 197 M. Farokhi, F. Mottaghitalab, Y. Fatahi, A. Khademhosseini and D. L. Kaplan, Overview of Silk Fibroin Use in Wound Dressings, *Trends Biotechnol.*, 2018, 36(9), 907–922.
- 198 D. N. Rockwood, R. C. Preda, T. Yucel, X. Q. Wang, M. L. Lovett and D. L. Kaplan, Materials fabrication from Bombyx mori silk fibroin, *Nat. Protoc.*, 2011, 6(10), 1612–1631.
- 199 A. P. Kishan and E. M. Cosgriff-Hernandez, Recent advancements in electrospinning design for tissue engineering applications: A review, *J. Biomed. Mater. Res., Part A*, 2017, 105(10), 2892–2905.
- 200 E. S. Pimentel, R. Brito-Pereira, T. Marques-Almeida, C. Ribeiro, F. Vaz, S. Lanceros-Mendez and V. F. Cardoso, Tailoring Electrospun Poly(L-lactic acid) Nanofibers as Substrates for Microfluidic Applications, *ACS Appl. Mater. Interfaces*, 2020, 12(1), 60–69.
- 201 C. Chen, B. T. Mehl, S. A. Sell and R. S. Martin, Use of electrospinning and dynamic air focusing to create three-dimensional cell culture scaffolds in microfluidic devices, *Analyst*, 2016, 141(18), 5311–5320.
- 202 C. P. Chen, A. D. Townsend, E. A. Hayter, H. M. Birk, S. A. Sell and R. S. Martin, Insert-based microfluidics for 3D cell culture with analysis, *Anal. Bioanal. Chem.*, 2018, 410(12), 3025–3035.
- 203 C. Chen, A. D. Townsend, E. A. Hayter, H. M. Birk, S. A. Sell and R. S. Martin, Insert-based microfluidics for 3D cell culture with analysis, *Anal. Bioanal. Chem.*, 2018, 410(12), 3025–3035.